



Waste water treatment by advanced oxidation processes (solar photocatalysis in degradation of industrial contaminants)

Sixto Malato

Plataforma Solar de Almería-CIEMAT. Carretera Senés km4, Tabernas (Almería). 04200-
Spain. Telf. 34- 950387940. Fax. 34-950365015. e-mail: sixto.malato@psa.es

Course on:

**Innovative Processes and Practices for Wastewater Treatment
and Re-use**

8-11 October 2007, Ankara University, Turkey

Waste water treatment by advanced oxidation processes (solar photocatalysis in degradation of industrial contaminants)

Plataforma Solar de Almería-CIEMAT. Carretera Senés km4, Tabernas (Almería). 04200-Spain. Telf. 34- 950387940. Fax. 34-950365015. e-mail: sixto.malato@psa.es

1. INTRODUCTION

The main causes of surface and groundwater contamination are industrial effluents (even in small amounts), excessive use of pesticides, fertilizers (agrochemicals) and domestic waste landfills. Wastewater treatment (WW) is usually based on physical and biological processes. After elimination of particles in suspension, the usual process is biological treatment (natural decontamination). Unfortunately, some organic pollutants, classified as bio-recalcitrant, are not biodegradable. In the near future, Advanced Oxidation Processes (AOPs) may become the most widely used water treatment technologies for organic pollutants not treatable by conventional techniques due to their high chemical stability and/or low biodegradability [1-4]. These processes involve generation and subsequent reaction of hydroxyl radicals ($\cdot\text{OH}$), which are one of the most powerful oxidizing species. Many oxidation processes, such as TiO_2/UV , $\text{H}_2\text{O}_2/\text{UV}$, Photo-Fenton and ozone (O_3 , O_3/UV , $\text{O}_3/\text{H}_2\text{O}_2$) are currently employed for this purpose. Their attack is not very selective, which is a useful attribute for use in pollution treatment. The versatility of AOPs is also enhanced by the fact that there are different $\cdot\text{OH}$ radical production possibilities, so they can be adapted to specific treatment requirements. Their main disadvantage is their high cost. The use of AOPs for WW treatment has been studied extensively, but UV radiation generation by lamps or ozone production is expensive [5]. So future applications of these processes could be improved through the use of catalysis and solar energy. Therefore, research is focusing more and more on those AOPs which can be driven by solar irradiation, photo-Fenton and heterogeneous catalysis with UV/TiO_2 . Several reviews have appeared during the last few years [6-12] and a especial effort has been made to supplement these reviews (not repeat information). Photo-Fenton combines Fenton (addition of H_2O_2 to Fe^{2+} salts) and UV-Vis light. Photolysis of Fe^{3+} complexes allows Fe^{2+} to be regenerated producing additional radicals and Fenton reactions to take place in the presence of H_2O_2 . Under these conditions, iron can be considered a real catalyst. Hydroxyl radicals can also be generated with a solid semiconductor that absorbs radiation (according to its band-gap) when in contact with water and generates pairs of valence-band holes and conduction-band electrons. Electron/ hole pairs (e^-/h^+) are generated by the absorption of photons with energy greater than necessary to move an electron from the valence band to the conduction band of the semiconductor. When electron/hole pairs are generated, the electron moves away from the surface to the bulk of the semiconductor as the hole migrates towards the surface. If the solvent is oxidoreductively active (water) it also acts as a donor and acceptor of electrons. Thus, on a hydrated and hydroxylated semiconductor surface, the holes produce $\cdot\text{OH}$ radicals. Whenever different semiconductor materials have been tested under comparable conditions for the degradation of the same compounds, TiO_2 has generally been demonstrated to be the most active. Since 1976, photocatalytic detoxification has been discussed in the literature as an alternative method for cleaning up polluted water [13] but industrial/commercial applications with solar energy, engineering systems and engineering design methodologies have only been developed recently [14]. This paper summarizes engineering work and recent developments in this area during the last few years.

2. SOLAR COLLECTORS FOR PHOTOCATALYTIC APPLICATIONS

2.1 Concentrating collectors

Contrary to solar thermal processes, which collect large amounts of photons at any wavelength to reach a specific temperature range, solar photochemical processes use only high-energy short-wavelength photons. TiO_2 photocatalysis uses UV or near-UV sunlight (300 to 400 nm) and photo-Fenton heterogeneous photocatalysis uses sunlight up to 580 nm. Sunlight at wavelengths over 600 nm is normally not useful. Nevertheless, the specific hardware needed for solar photocatalytic applications has much in common with those used for thermal applications. As a result, both photochemical systems and reactors have followed conventional solar thermal collector designs, such as parabolic troughs and non-concentrating collectors [21].

The original solar photoreactor designs [22] for photochemical applications were based on line-focusing parabolic-trough concentrators (PTCs). The parabolic-trough collector consists of a structure that supports a reflective concentrating parabolic surface (Figure 1). This structure has one or two motors controlled by a solar tracking system on one or two axes respectively that keep the collector aperture plane perpendicular to the solar rays. In this situation, all the solar radiation available on the aperture plane is reflected and concentrated on the absorber tube that is located at the geometric focal line of the parabolic trough. The first outdoor engineering-scale reactor developed was designed and built at the National Solar Thermal Test Facility at the Sandia laboratories in Albuquerque, New Mexico (USA), in 1989 (Figure 1, right). The facility was made up of 6 aligned parabolic-trough collectors with single-axis solar tracking for a total of 465 m^2 aperture area. The collector concentrated the sunlight about 50 times on the photoreactor [23, 24].

In 1990, a similar facility designed using PTCs and built at the Plataforma Solar de Almería, was the first engineering-scale solar photochemical facility for water detoxification in Europe [25] (Figure 1, left). It was made up of 12 two-axis solar-tracking parabolic-trough collectors, each having a total of 32 mirrors in 4 parallel parabolas with a collecting area of 32 m^2 .

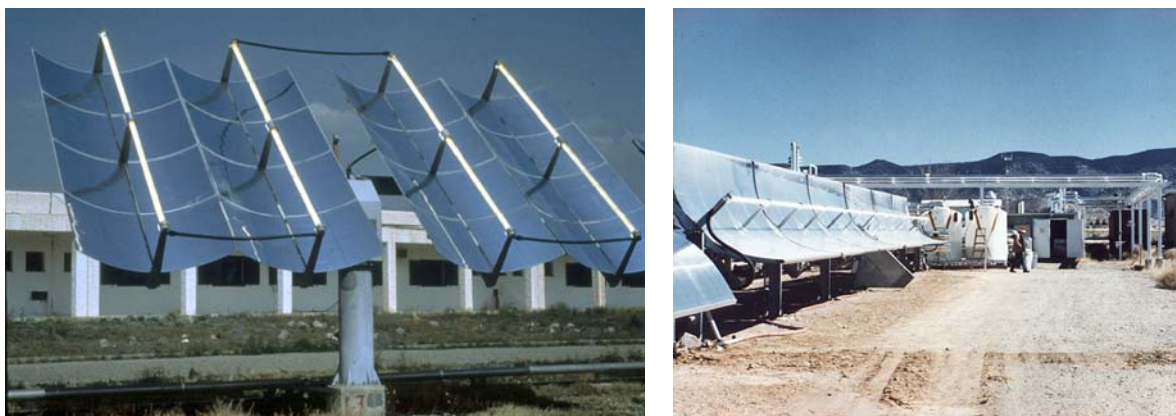


Figure 1. Parabolic-troughs with two-axis solar tracking (left) and single-axis solar tracking (right).

The solar radiation that reaches ground level without being absorbed or scattered, is called direct radiation, while radiation which has been dispersed before reaching the ground is called diffuse radiation, and the sum of both is called global radiation. Figure 2 shows the path of direct solar radiation (I_D) until it arrives inside the absorber tube. It must arrive at the surface and be reflected (part is lost due to mirror reflectivity, $\eta_{R,\lambda}$) in the right direction (here

affected by accurate sun tracking, η_s) by the mirror, before penetrating (part is lost due to glass transmissivity, $\eta_{T,\lambda}$) in the tube. Furthermore, the parabolic trough concentration factor must also be considered (ratio of surface area of the parabola capturing the radiation and surface area of the tube, S_p/S_T). Global radiation (I_G) is also collected by the PTCs, but global radiation is collected directly by the transparent absorber tube without intervention of the collector and is only affected by the transmissivity of the glass, $\eta_{T,\lambda}$.

All the details of these first developments were included several years ago in an excellent review by [22], and the main results were recently reviewed by [6]. Later, at the beginning of the nineties, attempts were made to use non-concentrating solar collectors as an alternative to PTCs, because PTCs are unsuitable for photocatalytic applications for several reasons [26]: water is heated, radiation flux is too high, most of the photons are not used efficiently [27-30] and their cost is high. The main advantages and disadvantages of these collectors are summarized in Table 1. Among other advantages, when supported catalysts are used in these collectors, a smaller amount can be used, as the photoreactor is smaller than in non-concentrating systems for the same solar collector area. Similarly, fewer tubes (smaller photoreactor tube area) are needed.

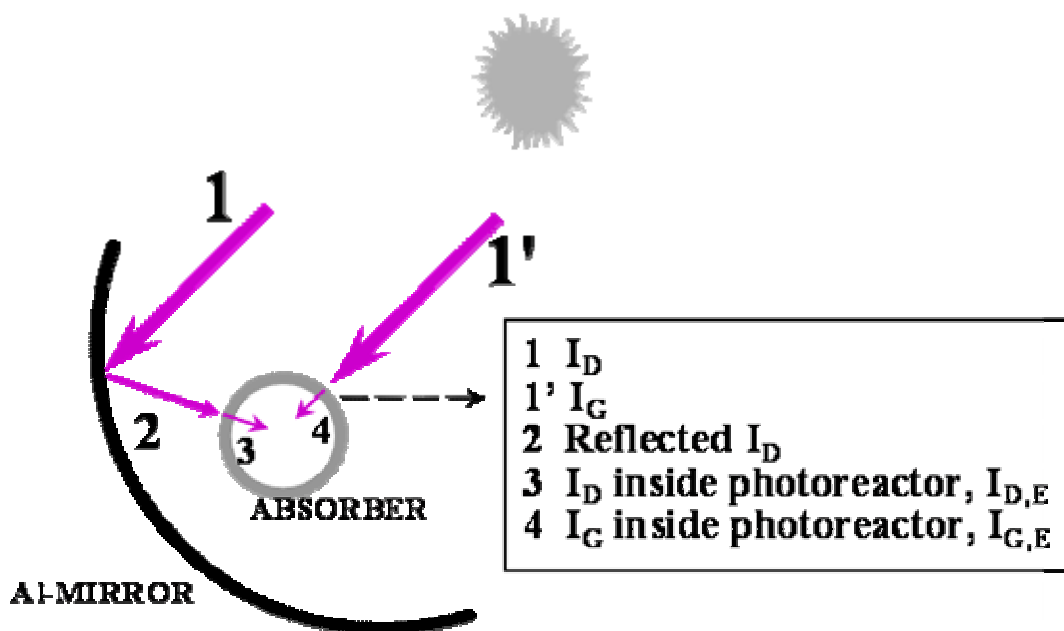


Figure 2. Photon flux (I) inside a parabolic-trough collector photoreactor.

2.2 Non-concentrating collectors

One-sun (non-concentrating) collectors are, in principle, cheaper than PTCs, as they have no moving parts or solar tracking devices [31]. They do not concentrate radiation, so efficiency is not reduced by factors associated with concentration and solar tracking. Manufacturing costs are cheaper because their components are simpler, which also means easy, low-cost maintenance. Non-concentrating collector support structures are easier and cheaper to install as well, and the surface required for their installation is smaller, because, since they are stationary, there is no shading. They are able to make use of the diffuse as well as the direct solar UV-A. Extensive effort in the design and testing of small non-tracking collectors has resulted in several different non-concentrating solar reactor prototypes. Most of this work has already been reviewed by our group [6] and only a few papers have been published since then about non-concentrating collectors [32-40]. One example of a non-

concentrating collector is shown in Figure 3. It consists of a rectangular stainless-steel staircase vessel having 21 steps. The photoreactor is provided with a Pyrex glass (UV-transparent) cover to limit water evaporation. The photoreactor, with a solar radiation-collecting surface of 1 m², is mounted on a fixed rack tilted at the same angle as the latitude of the site.

	ADVANTAGES	DISADVANTAGES
Concentrating collectors	- Turbulent flow	- Only direct radiation
	- No vaporization of compounds	- High cost (sun tracking)
	- More practical use of a supported catalyst	- Low optical efficiency
	- Smaller reactor tube area	- Low quantum efficiency ($r = k I^{-1}$ with TiO ₂) - Water overheating
Non concentrating photoreactors	- Direct and diffuse radiation	- Laminar flow (low mass transfer)
	- No heating	- Vaporization of reactants
	- Low cost	- Reactant contamination
	- High optical efficiency	- Weather resistance, chemical inertness and ultraviolet transmission
	- High quantum efficiency ($r = k I$ with TiO ₂)	

Table 1. Comparison between parabolic and non-concentrating solar photoreactors

Although one-sun collector designs possess important advantages, the design of a robust one-sun photoreactor is not trivial, due to the need for weather-resistant and chemically inert ultraviolet-transmitting reactors. In addition, non-concentrating systems require significantly more photoreactor area than concentrating photoreactors and, as a consequence, full-scale systems (normally composed of hundreds of square meters of collectors) must be designed to withstand the operating pressures anticipated for fluid circulation through a large field. Finally, its construction must be economical and should be efficient, with a low pressure drop. As a consequence, the use of tubular photoreactors has a decisive advantage because of the inherent structural efficiency of tubing. Tubing is also available in a large variety of materials and sizes and is a natural choice for a pressurized fluid system. Based on all of the above, reports by several different authors [11, 41-49] and experience acquired by the authors [27, 50-53], the main advantages and disadvantages of each of the different technologies for solar photocatalytic applications are as summarized in Table 1. Among other advantages, it should be mentioned that they use not only direct radiation but also diffuse radiation. As there is no concentrating system (with its inherent reflectivity), the optical efficiency is higher than for PTCs. In uncovered, non-concentrating systems exposed to the ambient, reactants could become contaminated. Very often the chemical inertness of the materials used (to resist corrosion caused by outdoor operation and exposure to solar irradiation) for constructing the non-concentrating collector should be guaranteed.

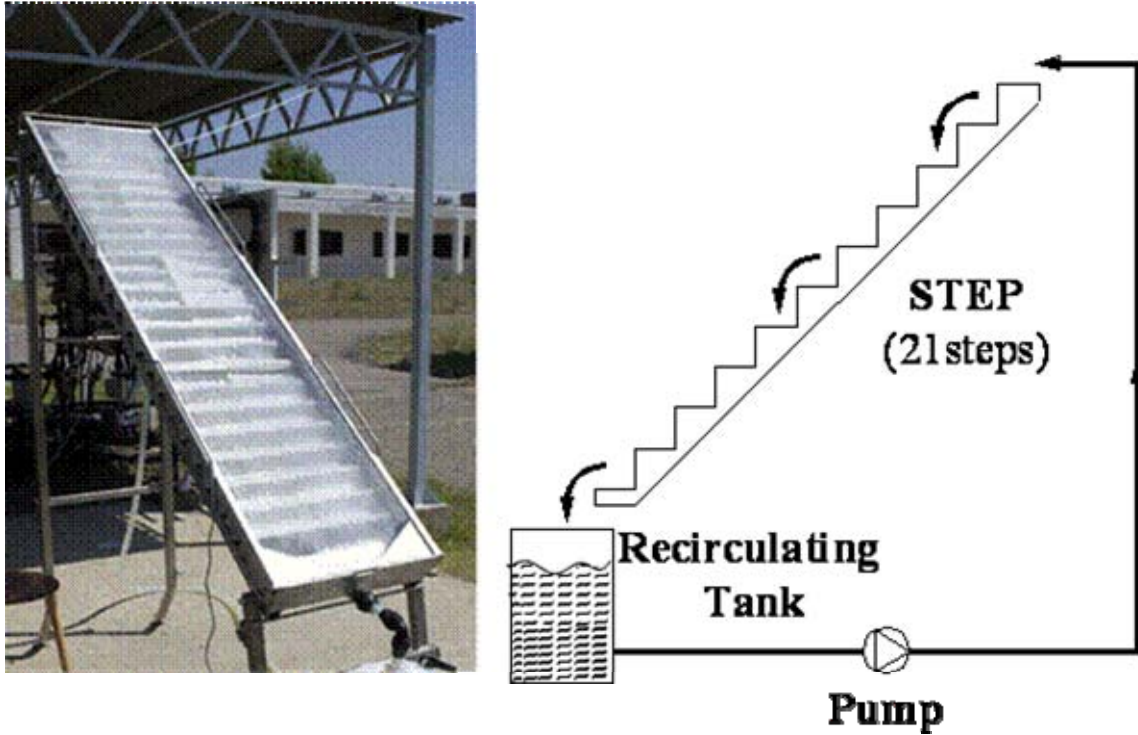


Figure 3. Non-concentrating solar collector tested at Plataforma Solar de Almería (Spain). Latitude 37 °N [39].

2.3 Compound parabolic concentrator (CPC)

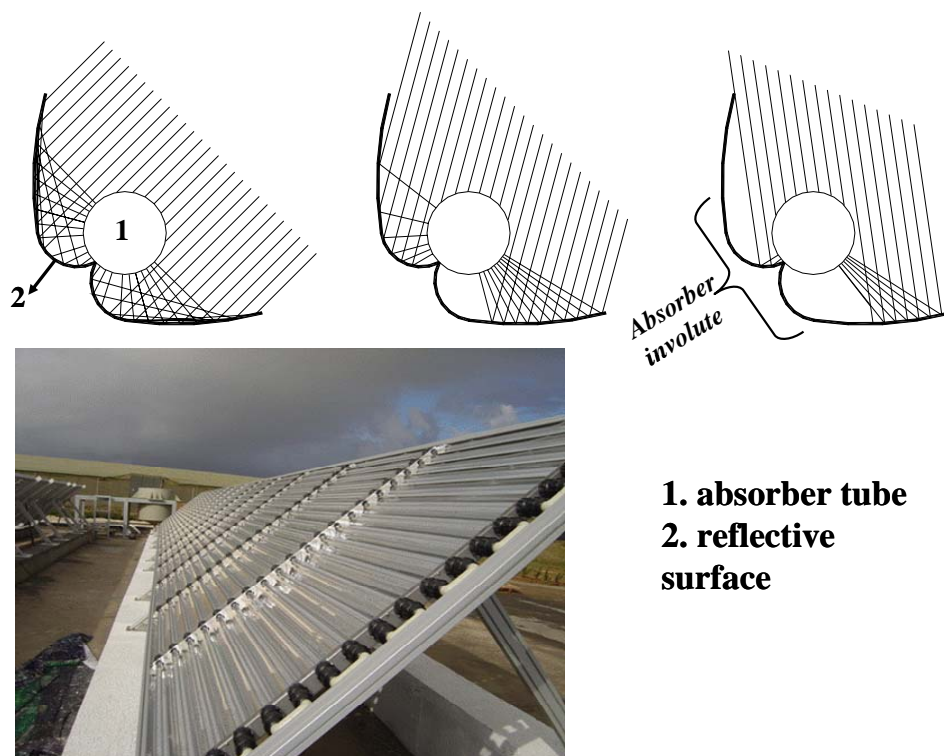
Compound Parabolic Concentrators (CPCs), a type of low-concentration collector used in thermal applications [54], is an option of interest. Between parabolic concentrators and flat stationary systems, they combine the characteristics of both. While they concentrate solar radiation, they retain the stationary and diffuse-radiation collection properties of flat plate collectors. They have therefore been chosen as a good option for solar photochemical applications by various research groups [45, 47, 55-65]. Summarizing, the advantages of CPCs are their turbulent flow conditions, no vaporization of volatile compounds, no tracking, no overheating, they can make use of both direct and diffuse solar radiation, are low-cost, weatherproof, reactants are not contaminated, and they have both high optical and high quantum efficiency, since there is a lower e^-/h^+ density than in a concentrating system (as the photonic density is lower) and therefore recombination is also lower. Having the advantages of both non-concentrating and concentrating systems and none of the disadvantages, CPCs seem to be the best option for solar photocatalytic processes.

The reason for this is that they illuminate the complete perimeter of the receiver, rather than just the "front" of it, as in conventional flat plates or tubes laid side by side (very often used as non-concentrating collectors in solar photocatalysis). The concentration factor (C_{CPC}) of a two-dimensional CPC collector is given by Eq. 1.

$$C_{CPC} = \frac{1}{\sin \theta_a} = \frac{a}{2\pi r} \quad (1)$$

The semi-angle of acceptance (θ_a) for photocatalytic applications is usually between 60 and 90 degrees. A special case is the one in which $\theta_a = 90^\circ$, whereby $C_{CPC} = 1$ (non-concentrating solar system), and each CPC curve is an ordinary involute (Figure 4). When this

occurs, all the UV radiation that reaches the aperture area of the CPC (direct and diffuse) can be collected and redirected to the reactor [53, 66]. If the CPC is designed for an acceptance angle of $+90^\circ$ to -90° , all of the diffuse solar radiation incident on the collector plane also impinges directly or indirectly on the photoreactor tube. The light reflected by the CPC is distributed all around the tubular receiver (Figure 4) so that almost the entire circumference of the receiver tube is illuminated and the light incident on the photoreactor is the same as would impinge on a flat plate.



1. absorber tube
2. reflective surface

Figure 4 Schematic drawing and photograph of a compound parabolic concentrator (see also Figure 8).

3. SOLAR PHOTOCATALYTIC DEGRADATION OF CONTAMINANTS

Solar photocatalysis aims at mineralizing the contaminants into carbon dioxide, water and inorganics, and treatment of industrial waste water seems to be one of the most promising fields of application of solar photocatalysis, however, each case is completely different [67, 68]. Consequently, preliminary research is always required to assess potential pollutant treatments and optimize the best option for any specific problem on a case-by-case basis. The following paragraphs summarize the main scientific articles that have appeared on this subject during recent years, all of them using solar energy as the photon source.

In photodegradation, the parent organic compound is transformed to eliminate its toxicity and persistence. The oxidation of carbon atoms into CO_2 is relatively easy. In general, however, it is markedly slower than the dearomatization of the molecule. Until now, the absence of total mineralization has been observed only in s-triazine herbicides, for which the final product obtained was essentially 1,3,5-triazine-2,4,6, trihydroxy (cyanuric acid), which is, fortunately, nontoxic [69]. This is because the triazine nucleus is so highly stable that it resists most methods of oxidation. Cl^- ions are easily released into the solution from chlorinated molecules [70-72]. Nitrogen-containing molecules are mineralized mostly into NO_3^- and NH_4^+ . Ammonium ions are relatively stable, and the proportion depends mainly on

the amount of oxidation of organic nitrogen and irradiation time [73-74]. Organophosphorous contaminants (mainly pesticides) produce phosphate ions. However, in the pH range used (usually < 4), phosphate ions remain adsorbed on TiO₂. This strong adsorption somewhat inhibits the reaction rate, though it is still acceptable [75]. In photo-Fenton, phosphate sequesters iron forming the corresponding non-soluble salt and retarding the reaction rate. Therefore, more iron is necessary when water containing phosphates is treated by photo-Fenton [76]. Until now, the analyses of fragments resulting from the degradation of the aromatic ring have revealed formation of aliphatics (organic acids and other hydroxylated compounds), which explains why total mineralization takes much longer than dearomatization [77-81], as mineralisation of aliphatics is the slowest step.

Special attention has recently been given the so called “emerging contaminants”, mostly unregulated compounds that may be candidates for future regulation depending on research on their potential effects on health and monitoring data regarding their occurrence [82]. Particularly relevant examples of such emerging compounds are surfactants, pharmaceuticals and personal care products, which do not need to persist in the environment to cause a negative effect, because their high transformation/removal rates can be compensated by their continuous introduction into the environment [83]. The solar photocatalytic degradation of these new environmental contaminants, many until recently unknown, is the focus of much research [84-88].

3.1 Improving solar photocatalysis efficiency

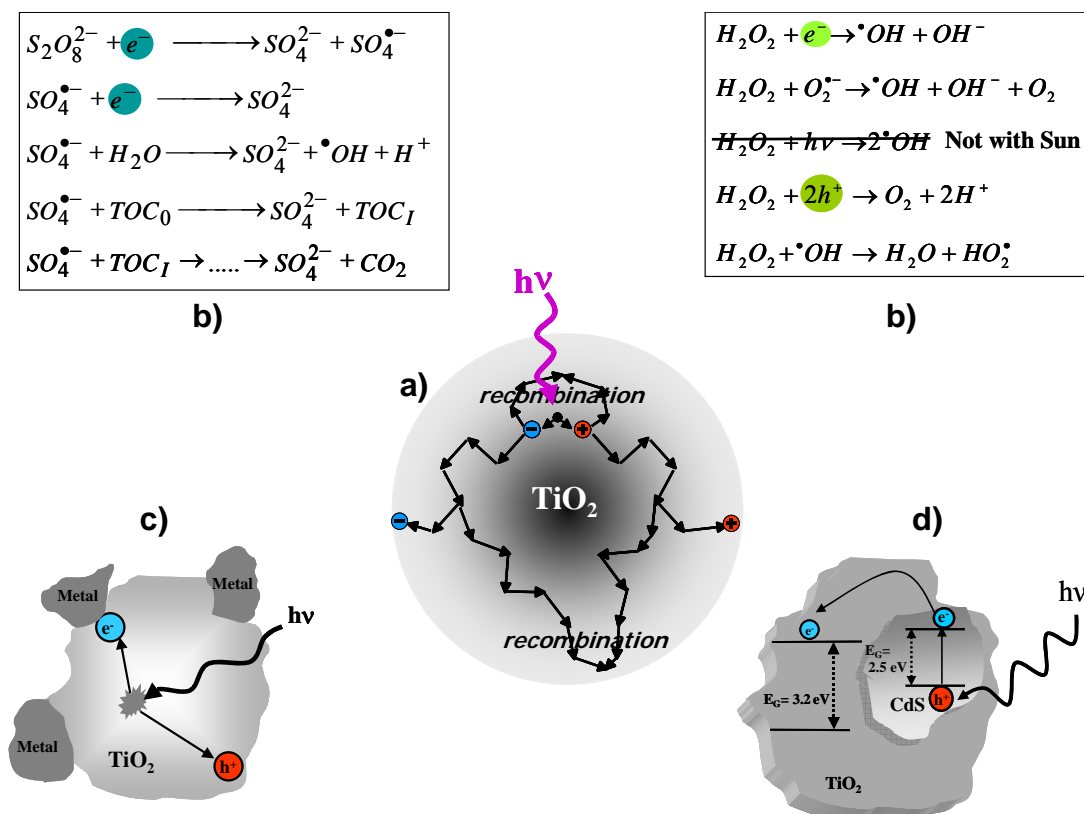


Figure 5. Electron/hole recombination (a) and ways of improving solar photocatalysis reaction rates: (b) Use of electron acceptors; (c) Electron capture by a metal in contact with a semiconductor surface; (d) Semiconductor-semiconductor photocatalyst.

However, as concentration and number of contaminants increase (as in real waste water with complex mixtures of organics), the process becomes more complicated and challenging problems such as slow kinetics caused mainly by low photoefficiency need to be solved. Electron/hole recombination (Figure 5a) in the absence of proper electron acceptors, is extremely efficient and thus represents a major energy-wasting step and quantum yield limiting factor. Besides, the TiO₂ band-gap represents only 5% of the solar spectrum. It is therefore a rather inefficient process even for a high-added-value application. Two basic lines of R&D have been working on modifying catalyst structure and composition (Figure 5c) and addition of electron acceptors to increase the solar photocatalytic reaction rate (Figure 5b). A third approach has focused on finding new catalysts able to work with band-gaps which coincide better with (Figure 5d) the solar spectrum [89-92]. There have been many attempts using the first and third approach, such as improving specific surface [39, 68, 93, 94] by doping and deposition with metal ions and oxides [95-98]. Successful innovative catalyst compositions have been developed, but they have not been used in large-sized plants because no “cheap” solution has yet been developed. Our experience in testing at large solar facilities with different contaminants qualifies the use of electron acceptors as the most versatile way of improving reaction rates for now, opening the opportunity for extending the use of heterogeneous photocatalysis to complicated waste water [99-102].

3.2 Combining solar photocatalysis and biotreatment

Apart from developments increasing the photocatalytic reaction rate, the most important progress in solar photocatalysis in recent years has been related to its combination with biological treatment and the application of toxicological analytical methods. Both approaches have been successful in decreasing treatment time (i.e. plant size), which is another way of increasing overall process efficiency, in contrast to increasing the reaction rate itself. Contaminant treatment, in its strictest meaning, is the complete mineralisation (TOC = 0) of the contaminants, however, today photocatalytic processes only make sense for nonbiodegradable hazardous pollutants. When feasible, biological treatment is usually a good solution. Therefore, biologically recalcitrant compounds could be treated with photocatalytic technologies until biodegradability is achieved and then the water would be discharged to a conventional biological plant. One of the main obligations for urban wastewater treatment imposed by European Union Council Directive 91/271/EEC is that wastewater collecting and treatment systems (generally involving biological treatment) should be provided by 31 December 2005 in all agglomerations of between 2000 and 15000 p.e. (population equivalent). The deadline for agglomerations of more than 15000 p.e. should have been met by the end of 2000 [103]. Therefore, in the near future, most of the AOP plants developed in the EU could discharge pre-treated wastewater into a nearby conventional biological treatment, without the necessity of installing a specific biotreatment coupled to the AOP. Future evaluation of AOP efficiency should therefore be done from this perspective, instead of attempting to completely mineralise the contaminants using the $\cdot\text{OH}$ radicals, which is always more expensive. Such a combination reduces treatment time and optimizes the overall economics, since the solar detoxification system can be significantly smaller [61, 104, 105]. Process kinetics make the first part of the photocatalytic treatment the quickest. It may be observed in Figure 6 that most of the DPs (degradation products) with high molecular weight appear after exposure to sunlight and reach their maximum concentration after around 10 min of treatment. From here on, they begin to decrease and carboxylic acids appear. In any case, and for purposes of wastewater treatment, the complete mineralisation by photocatalysis is unnecessary in view of the DPs detected, because they could easily be treated in a conventional biological treatment plant.

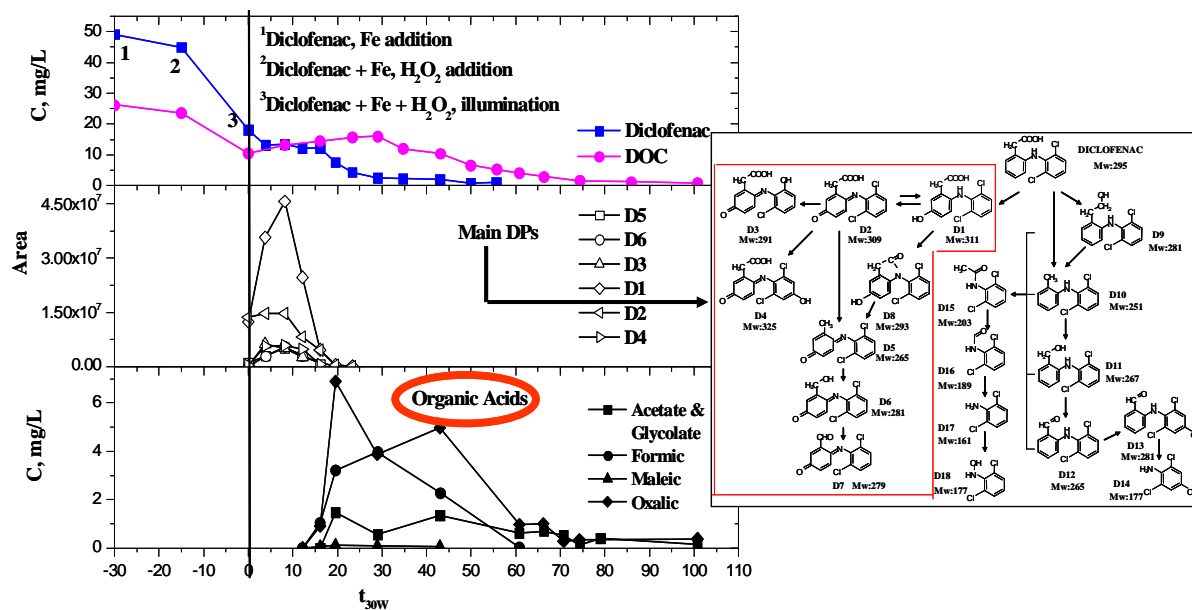
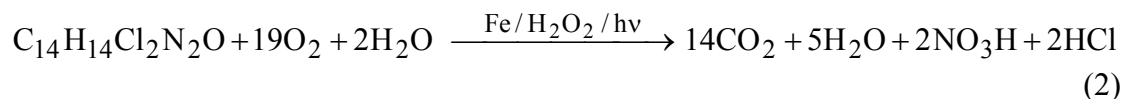


Figure 6. Evolution over time of the main degradation products and carboxylic acids detected during solar photocatalytic treatment of diclofenac (non-steroidal anti-inflammatory drug considered an “emerging contaminant”). Taken from [88].

Therefore, the use of AOPs as a pretreatment can be justified if the intermediates resulting from the reaction (more oxidized compounds, such as carboxylic acids, alcohols, etc) are readily degraded by microorganisms. The feasibility of such a photocatalytic-biological process combination must always be considered, as it could mean a significant cost reduction due to the smaller solar collector field necessary. Biotreatment and solar photocatalysis combination has only been developed recently, and there are not many papers on the subject [63, 106-110]. An “on-going” project (“A Coupled Advanced Oxidation–Biological Process for Recycling of Industrial Wastewater Containing Persistent Organic Contaminants”, CADOX) sponsored by the European Commission and with the participation of nine EU partners (<http://www.psa.es/webeng/projects/cadox/index.html>), focusing on this new hybrid technology, attempts to demonstrate how the treatment cost of water containing persistent contaminants can be drastically reduced. Figure 7 and Table 2 show an example of evaluation of photo-Fenton treatment of real waste water containing a pesticide (imazalil) taking into account biodegradability results. The overall reaction (Eq. 2) for oxidation of imazalil shows that inorganic species produced are nitrate and chloride. As clearly shown in Figures 7, when imazalil has disappeared ($t = 45$ min and $t = 90$ min by $Fe = 0.5$ mM and $Fe = 0.1$ mM, respectively), mineralisation is still very low.



Chloride analyses (determined during degradation of chlorinated compounds) showed very fast degradation/dechlorination compared to disappearance of TOC. Therefore, residual TOC remaining in the water when imazalil has completely disappeared did not correspond to any chlorinated compound. In order to find out the conditions for biocompatibility using the photo-Fenton reaction as a pre-treatment step, the biodegradability of the wastewater was evaluated by the BOD₅ (Biochemical Oxygen Demand) test, using unacclimated municipal sludge as the initial inoculum. The results are shown in Table 2. Different stages of the treatment were taken as the reference for the biocompatibility study. It should be noted that

complete disappearance of imazalil and chloride release were considered the key-parameter for selection of the treatment stage to be tested by BOD₅. Table 2 shows that there was some degradation of imazalil intermediates by the microorganism in all cases, after pesticide disappearance. It may easily be concluded that biodegradability is enhanced during the treatment (BOD/COD ratio), although biodegradability was better if the treatment was not excessively prolonged (compare Samples 3 and 4). In view of these results, and to the intrinsic uncertainty of biodegradable methods, the best value for discharging waste water to a biotreatment could be set within a wide interval between 195 mg/L and 35 mg/L of TOC. The most suitable conditions for biotreatment are therefore obtained when the phototreatment time is just long enough for high biological efficiency (not too much mineralisation so the effluent has a high enough biodegradable organic charge). Longer phototreatment times produce unnecessary photodegradation of biologically degradable substances, and higher energy consumption uncompensated by any benefit.

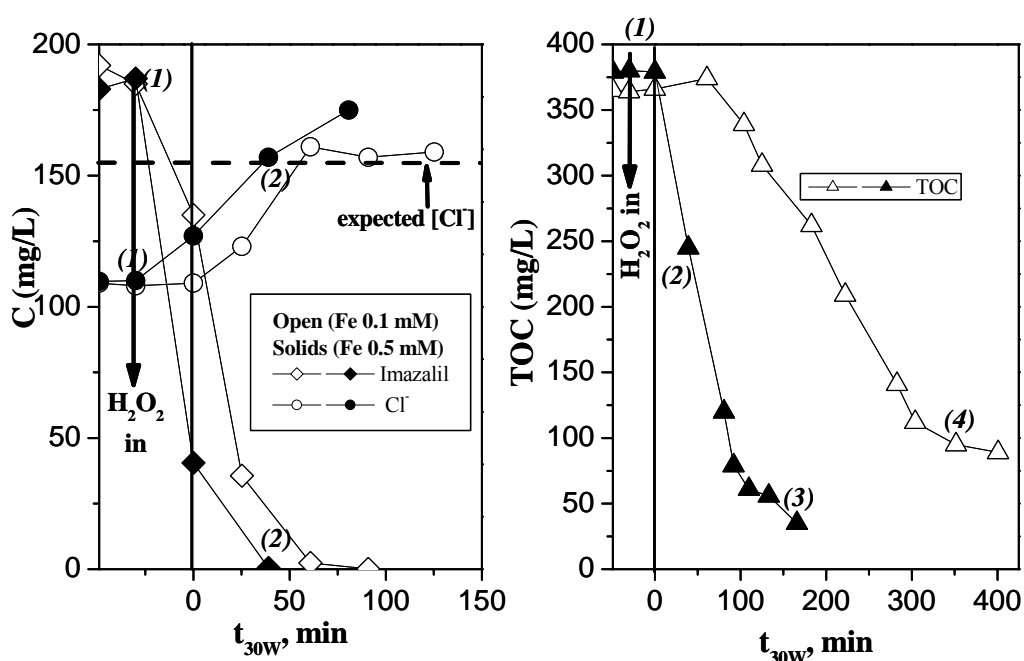


Figure 7. Disappearance of imazalil and evolution of chloride and total organic carbon (TOC) as a function of illumination time during photo-Fenton treatment of real wastewaters (see Table 2). Points 1-4 refer to data shown in Table 2.

	(1)	(2)	(3)	(4)
COD (mg/L)	950	384	82	119
BOD (mg/L)	0.00	123	36.9	64.3
BOD/COD ratio:	0.00	0.32	0.45	0.54
BOD/COD rating:	Very poor	good	good	Very good
Imazalil (mg/L)	199.8	<0.1	<0.1	<0.1
Conductivity (mS/cm)	1.61	2.55	2.44	2.89
Cl ⁻ (mg/L)	105	164	161	163
TOC (mg/L)	285	195	34.6	93.9

Table 2. Main characteristics of real wastewater containing imazalil (1) and after photo-Fenton treatment at different stages (2, 3 and 4). Photo-Fenton experiments shown in Figure 7.

4. INSTALLED SOLAR PHOTOCATALYTIC TREATMENT PLANTS

Despite its obvious potential for the detoxification of polluted water, there has been very little commercial or industrial use of photocatalysis as a technology to date. Several years ago, according to a review by Goswami [21], only two engineering-scale demonstrations, one for groundwater treatment in the U.S. and one for industrial wastewater treatment in Spain (at Plataforma Solar de Almería) had been published. But more installations have recently been erected, mainly based on non-concentrating collectors. Dillert et al. have treated biologically pretreated industrial waste water from the Volkswagen AG factories in Wolfsburg (Germany) and Taubaté (Brazil). The results of the experiments, which were performed using the Double Skin Sheet Reactor (DSSR) [111], were so promising, that a pilot plant was installed in the Wolfsburg factory during the summer of 1998 [112]. The flowchart of a more recent version of this pilot plant, which was installed in 2000, has recently been published by Bahnemann [8]. In 1997, Freudenhammer et al. reported their results from a pilot study with the TFFBR (Thin Film Fixed Bed Reactor) in various Mediterranean countries [113, 114]. Based on these results, a pilot plant, financed by the European Commission, has been built at the site of a textile factory in Tunisia (Menzel Temime). The pilot plant description and the flow chart have recently been published [8; 36].

Under the “SOLARDETOX” project (Solar Detoxification Technology for the Treatment of Industrial Non-Biodegradable Persistent Chlorinated Water Contaminants), a consortium coordinated by Plataforma Solar de Almería, Spain, was formed in Europe for the development and marketing of solar detoxification of recalcitrant water contaminants [115]. The main goal of the project (financed by the EC-DGXII through the Brite Euram III Program, 1997–2000) was to develop a commercial non-concentrating solar detoxification system using the compound parabolic collector technology (CPC), with a concentration ratio = 1. A full-size demonstration plant for field demonstration to identify any pre- or post-processing requirements, potential operating problems, and capital and operating costs [115] was erected at the facilities of HIDROCEN (Madrid, Spain). Since late 1999, this plant, (main characteristics and results published elsewhere [116]), including the catalyst separation procedure also developed under the SOLARDETOX project and installed for the first time in this plant, has been fully operative [117]. The same collectors have also been used by other researchers for treating paper mill effluents in Brazil and Germany [62, 118-120], and paper mill effluents [64], surfactants [121], and textile dyes [65] in Spain.

More recently (2004), a new CPC-based plant, has been installed (Figure 8) in a project focusing on problems in the rapidly growing intensive greenhouse agriculture sector in the Mediterranean Basin. The environmental problems caused are one of its greatest disadvantages. One of these problems is the uncontrolled dumping of plastic pesticide containers, which usually still contain residues. The solution is to selectively collect these containers for recycling. Plastic container recycling starts with shredding and then industrial washing of the shredded plastic, which produces water polluted with highly toxic persistent compounds (pesticides + excipients). This hazardous water containing the dissolved toxic organic matter that was in the pesticide containers must be treated. This rinse water is then continuously recycled and reused. The ALBAIDA company and CIEMAT (Spain) jointly presented a project entitled “Environmental Collection and Recycling of Plastic Pesticide Bottles using Advanced Oxidation Process driven by Solar Energy” to the European LIFE-ENVIRONMENT program, which was approved and began in October 2001. The plant is now in routine operation.

The photo-Fenton treatment mineralizes 80% of the TOC in the rinse water in a batch process. The plant design, based on CPC solar collectors (150 m²), has 4 parallel rows of 14

photocatalytic reactor modules (20 tubes/module, 2.7 m²/module) mounted on a 37°-tilted platform (local latitude). The total collector surface is 150 m² and total photo reactor volume is 1060 L. The 14 modules in each row are connected in series so the water flows from one module to another and finally to a tank. However, each row is independent and connected in parallel, so they can be operated separately. The system is run in batch mode using a recirculation tank with only one centrifugal pump. The treated water from washing plastic pesticide bottles is returned to the washing system by a second pump and the system can again be refilled with contaminated water from the bottle-washing plant. Before entering the solar CPC field, solids are eliminated from the contaminated water and the reagents needed (hydrogen peroxide and Fe²⁺) for the photo-Fenton reaction are added. As the CPCs have a concentration factor of approximately 1 and there is no thermal insulation, the maximum temperature reached inside the photo reactor is around 40°C. After treatment, the Fe need not be removed because the water will either be reused or, when discharged, transferred to a 20,000-m³ irrigation pool where it is not only not a problem, but is an advantage, as it is one of the elements usually added to greenhouse irrigation water.



Figure 8 View of the solar detoxification demonstration plant erected by ALBAIDA at La Mojonera (Almería, Spain).

REFERENCES

- [1] P.R. Gogate and A.B. Pandit, *Adv. Environ. Res.*, 8 (2004) 501.
- [2] P.R. Gogate and A.B. Pandit, *Adv. Environ. Res.*, 8 (2004) 553.
- [3] I.K. Konstantinou and T.A. Albanis, *Applied Catal. B: Environ.*, 49 (2004) 1.
- [4] M. Pera-Titus, V. García-Molina, M.A. Baños, J. Giménez and S. Esplugas *Appl. Catal. B: Environ.*, 47 (2004) 219.
- [5] Muñoz, J. Rieradevall, F. Torrades, J. Peral and X. Domènech, *Solar Energy*, 79 (2005) 369.
- [6] S. Malato, J. Blanco, A. Vidal and C. Richter, *Appl. Catal. B: Environ.*, 37 (2002), 1.
- [7] I.K. Konstantinou and T.A. Albanis, *Applied Catalysis B: Environmental* 42 (2003), 319.
- [8] D. Bahnemann, *Solar Energy*, 77 (2004) 445.
- [9] D.Y. Goswami, S. Vijayaraghavan, S. Lu and G. Tamm, *Solar Energy*, 76 (2004) 33.
- [10] S. Devipriya and S. Yesodharan, *Sol. En. Mat. Sol. Cells*, 86 (2005) 309.
- [11] A.A. Adesina, *Catalysis Surveys from Asia*, 8 (2004) 265.
- [12] J.M. Herrmann, *Topics in Catalysis*, 14 (2005), 48.

- [13] J.H. Carey, J. Lawrence and H.M. Tosine, *Bull. of Environ. Contamination & Toxicol.*, 16 (1976) 697.
- [14] J. Blanco and S. Malato, *Solar Detoxification*, UNESCO Publishing, France, 2003.
- [15] Freuze, S. Brosillon, A. Laplanche, D. Tozza and J. Cavard, *Water Research*, 39 (2005) 2636.
- [16] E.T. Urbansky, and M.L. Magnuson, *Analytical Chemistry*, 74 (2002) 267.
- [17] W. J. Huang, G.-C. Fang and C. C. Wang, *Science of the Total Environment* 345 (2005) 261.
- [18] W.J. Masschelin, *Ultraviolet Light in Water y Wastewater Sanitation*, Lewis Publishers, Florida, 2002, p. 59.
- [19] L.L. Gyurek, G.R. Finch and M. Belosevic, *J. Environ. Engin.*, 123 (1997) 865.
- [20] T. Matsunaga, R. Tomoda, T. Nakajima and H. Wake, *FEMS Microbiol. Lett.*, 29 (1985) 211.
- [21] D.Y. Goswami, *J. Sol. En. Eng.*, 119 (1997) 101.
- [22] D.Y. Goswami, *Adv. in Solar Energy*, (1995) 165.
- [23] J.V. Anderson, H. Link, M. Bohn and B. Gupta, *Solar En. Mat.*, 24 (1991) 538.
- [24] M.R. Prairie, J.E. Pacheco and L.R. Evans, *Solar Eng.*, 1 (1992) 1.
- [25] Minero, E. Pelizzetti, S. Malato and J. Blanco, *Chemosphere*, 26 (1993) 2103.
- [26] O.M. Alfano, D. Bahnemann, A.E. Cassano, D. Dillert and R. Goslich, *Catalysis Today* 58 (2000) 199.
- [27] S. Parra, S. Malato, J. Blanco, P. Péringier and C. Pulgarin. *Wat. Sci. Technol.*, 44 (2001) 219.
- [28] T. Zhang, T. Oyama, S. Horikoshi, J. Zhao, H. Hidaka and N. Serpone, *Solar Energy*, 71 (2001) 305.
- [29] T. Oyama, A. Aoshima, S. Horikoshi, H. Hidaka, J. Zhao and N. Serpone, *Solar Energy*, 77 (2004) 525.
- [30] S. Gelover, P. Mondragón and A. Jiménez, *J. Photochem. Photobiol. A: Chem.*, 165 (2004). 241.
- [31] P. Wyness, J.F. Klausner, D.Y. Goswami K.S. Schanze, *J. Solar Energy Engineering*, 116 (1994) 2.
- [32] H. C. Chan, C.K. Chan, J.P. Barford and J.P. Porter, *Wat. Res.*, 37 (2003) 1125.
- [33] S. Kanmani, K. Thanasekaran and D. Beck, *Ind. J. Chem. Technol.*, 10 (2003) 638.
- [34] W. Gernjak, T. Krutzler, A. Glaser, S. Malato, J. Cáceres, R. Bauer and A. R. Fernández, *Chemosphere*, 50 (2003) 718.
- [35] W. Gernjak, M.I. Maldonado, S. Malato, J. Cáceres, T. Krutzler, A. Glaser and R. Bauer, *Solar Energy*, 77 (2004) 567.
- [36] L. Bousselmi, S. U. Geissen, and H. Schroeder, *Wat. Sci. Technol.*, 49 (2004) 331.
- [37] H. Rossetti, E. D., Albizzati and O. M. Alfano, *Solar Energy*, 77 (2004) 461.
- [38] P. Pichat, S. Vannier, J. Dussaud and J. P. Rubis, *Solar energy*, 77 (2004) 533.
- [39] Ch. Guillard, J. Disdier, Ch. Monnet, J. Dussaud, S. Malato, J. Blanco, M. I. Maldonado, and J.M. Herrmann, *Appl. Catal. B: Environ.*, 46 (2003) 319.
- [40] L. Zou, Y. Li and E. Hu, *J. Environ. Eng.*, 131 (2005) 102.
- [41] K. Pacheco, A. S. Watt and C. S. Turchi, *Sol. Eng.*, (1993) 43.
- [42] M., Srinivasan, D.Y. Goswami, J.F. Klausner and C.K. Jotshi, *Proc. ASME International Solar Energy Conference*, Albuquerque, New Mexico, 1998, p. 299.
- [43] R. Dillert, A. E. Cassano, R. Goslich and D. Bahnemann, *Catalysis Today*, 54 (1999) 267.
- [44] J. Giménez, D. Curcó and M.A. Queral, *Catalysis Today*, 54 (1999) 229.
- [45] J. A. Ajona and A. Vidal, *Solar Energy*, 68 (2000) 109.

- [46] E. R. Bandala, S. Gelover, M. T. Leal, C. Arancibia, A. Jimenez and C. A. Estrada, *Catalysis Today*, 76 (2002) 189.
- [47] E. R. Bandala, C. A. Arancibia, S. L. Orozco and C. A. Estrada, *Solar Energy*, 77 (2004) 503.
- [48] E. R. Bandala and C. A. Estrada, *J. Solar Energy Engineering*, in press (2006).
- [49] Claudio A.O. Nascimento, Antonio C.S.C. Teixeira, R. Guardani, Frank H. Quina, Osvaldo C. Filho and André M. Braun. *J. Solar Energy Engineering*, in press (2006).
- [50] Minero, E. Pelizzetti, S. Malato and J. Blanco, *Solar Energy*, 56 (1996) 421.
- [51] S. Malato, J. Gimenez, C. Richter, D. Curco and J. Blanco, *Wat. Sci. Techn.*, 35 (1997) 157-164.
- [52] M. Romero, J. Blanco, B. Sánchez, A. Vidal, S. Malato, A. Cardona and E. García, *Solar Energy*, 66 (1999) 169.
- [53] S. Malato, J. Blanco, M. I. Maldonado, P. Fernández, D. Alarcon, M. Collares, J. Farinha, and J. Correia, *Solar Energy*, 77 (2004) 513.
- [54] W.T. Welford and R. Winston, *The Optics of Non - Imaging Concentrators Light and Solar Energy*, Academic Press, 1978.
- [55] C.S. Turchi and M.S. Mehos, *Chem. Oxid.*, 2 (1994) 301.
- [56] K.-H. Funken, C. Sattler, B. Milow, L. de Oliveira, J. Blanco, P. Fernández, S. Malato, M. Brunotte, N. Dischinger, S. Tratzky, M. Musci and J.C. de Oliveira, *Wat. Sci. Technol.*, 44 (2001) 271.
- [57] B.A. Jubran, A.F., Ismail and T. Pervez, *Energy Conversion & Management*, 41 (2000) 1.
- [58] M. Kus, W. Gernjak, P. Fernández Ibáñez, S. Malato Rodríguez, J. Blanco Gálvez and S. Icli, *J. Solar Energy Engineering*, in press (2006)
- [59] G. Peñuela, G.M. Mejía, G. Hincapié, N. Cuervo, J. Marín and G.M. Restrepo, *Waste Management and the Environment* (2002) 321.
- [60] Robert and S. Malato, *Sci. Total Environ.*, 291 (2002) 85.
- [61] S. Malato, J. Blanco, A. Vidal, D. Alarcón, M. I. Maldonado, J. Cáceres and W. Gernjak, *Solar Energy*, 75 (2003) 329.
- [62] Sattler, K.-H. Funken, L. de Oliveira, M. Tzschirner and A.E.H. Machado, *Wat. Sci. Technol.*, 49 (2004) 189.
- [63] V. Sarria, S. Kenfack, O. Guillod and C. Pulgarin, *J. Photochem. Photobiol. A: Chem.*, 159 (2003) 89.
- [64] M. Amat, A. Arques, F. López, and M.A. Miranda, *Solar Energy*, 79 (2005) 393.
- [65] O. Prieto, J. Feroso, Y. Nuñez, J.L. del Valle and R. Hirsuta, *Solar Energy*, 79 (2005) 3763.
- [66] J. Chaves and M. Collares Pereira. *J. Solar Energy Engineering*, in press (2006)
- [67] S. Malato, J. Blanco, J. Cáceres, A. R. Fernández, A. Agüera and A. Rodríguez, *Catalysis Today*, 76 (2002) 209.
- [68] S. Malato, J. Blanco, A. Campos, J. Cáceres, C. Guillard, J.M. Herrmann and A. R. Fernández-Alba, *Appl. Catal. B: Environ.*, 42 (2003) 349.
- [69] M. Hincapié, M.I. Maldonado, I. Oller, W. Gernjak, J.A. Sánchez, M.M. Ballesteros and S., Malato, *Catalysis Today*, 101 (2005) 203.
- [70] R.F.P. Nogueira, A.G. Trovó nad D.F. Modé, *Chemosphere*, 48 (2002) 385.
- [71] J. Park, E. Choi, I.-H. Cho and Y.-G. Kim, *J. Environ. Sci. Health A*, 38 (2003) 1915.
- [72] S. Malato, J. Blanco, M. I. Maldonado, P. Fernández, W. Gernjak and I. Oller, *Chemosphere*, 58 (2005) 391.
- [73] V. Augugliaro, C. Baiocchi, A. Bianco, M.C. Brussino, E. García-López, V. Loddo, S. Malato, G. Marci, L. Palmisano and E. Pramauro, *Fresenius Environ. Bull.*, 11 (2002) 459.

- [74] V. Augugliaro, C. Baiocchi, A. Bianco, E. García-López, V. Loddo, S. Malato, G. Marci, L. Palmisano, M. Pazzi and E. Pramauro, *Chemosphere* 49 (2002) 1223.
- [75] Shifu and C. Gengyu, *Solar Energy*, 79 (2005) 1
- [76] Oller, W. Gernjak, M. I. Maldonado, P. Fernández, J. Blanco, J. A. Sánchez and S. Malato, *Environ Chem Lett*, 3 (2005) 118.
- [77] Agüera, M. Mezcua, D. Hernando, S. Malato, J. Cáceres and A. Fernández-Alba, *Intern. J. Environ. Anal. Chem.*, 84 (2004) 149.
- [78] Agüera, L. A. Perez Estrada, I. Ferrer, E. M. Thurman, S. Malato, and A. R. Fernandez-Alba, *J. Mass Spectrometry*, 40 (2005) 908.
- [79] V. Augugliaro, A. Bianco, J. Caceres, E. Garcia, A. Irico, V. Loddo, S. Malato, G. Marci, L. Palmisano and E. Pramauro, *Adv. Environ. Res.*, 8 (2004) 329.
- [80] V. Sarria, P. Péringier, J. Cáceres, J. Blanco, S. Malato and C. Pulgarin, *Energy*, 29 (2004) 853.
- [81] S. Malato, J. Cáceres, A. R. Fernández-Alba, L. Piedra, M. D. Hernando, A. Agüera and J. Vial, *Env. Sci. Technol.*, 37, (2003) 2516.
- [82] D. Barceló, *Trends Anal. Chem.*, 22 (2003) xiv.
- [83] R. Andreatti, M. Raffaele and P. Nicklas, *Chemosphere*, 50 (2003) 1319.
- [84] G. Mailhot, M. Sarakha, B. Lavedrine, J. Cáceres and S. Malato, *Chemosphere*, 49 (2002) 525.
- [85] J. Wiszniowski, D. Robert, J. Surmacz, K. Miksch, S. Malato and J.V. Weber, *Appl. Catal. B: Environ.*, 53 (2004) 127.
- [86] V. Augugliaro, E. Garcia, V. Loddo, S. Malato, M. I. Maldonado, G. Marci, R. Molinari, and L. Palmisano, *Solar Energy*, 79 (2005) 402.
- [87] L.A. Pérez, M.I. Maldonado, W. Gernjak, A. Agüera, A.R. Fernandez, M.M. Ballesteros and S. Malato, *Catalysis Today*, 101 (2005) 219.
- [88] L. A. Pérez-Estrada, S. Malato, W. Gernjak, A. Agüera, E. M. Thurman, I. Ferrer and A. R. Fernández-Alba, *Environ. Sci. Technol.*, 39 (2005) 8300.
- [89] D. Gryglik, J.S. Miller, S. Ledakowicz, *Solar Energy*, 77 (2004) 615.
- [90] M. Rios-Enriquez, N. Shahin, C. Durán, J. Lang, E. Oliveros, S H. Bossmann and A M. Braun, *Solar energy*, 77 (2004) 491.
- [91] D. Gumy, P. Fernandez, S. Malato, C. Pulgarin, O. Enea and J. Kiwi, *Catalysis Today*, 101 (2005) 375.
- [92] J. A., Rengifo, J. Sanabria, F. Machuca, C. F. Dierolf, C. Pulgarín and G. Orellana, *J. Solar Energy Engineering*, in press (2006).
- [93] J. M. Herrmann, Ch. Guillard, J. Disdier, C. Lehaut, S. Malato and J. Blanco, *Appl. Catal. B: Environ.*, 35 (2002) 281.
- [94] J. Trujillo, T. Safinski and A. A. Adesina, *J. Solar Energy Engineering*, in press (2006).
- [95] T. Sano, N. Negishi, K. Takeuchi and S. Matsuzawa, *Solar Energy*, 77 (2004) 543.
- [96] Sahoo, A.K. Gupta and A. Pal, *Dyes and Pigments*, 66 (2005) 189.
- [97] D., Li, H., Haneda, S., Hishita, N. Ohashi, *Res. Chem. Interm.*, 31 (2005) 331.
- [98] J. Araña, J. M. Doña Rodríguez, O. González Díaz, J. A. Herrera Melián and J. Pérez Peña, *J. Solar Energy Engineering*, in press (2006).
- [99] T. Zhang, T. Oyama, S. Horikoshi, J. Zhao, N. Serpone and H. Hidaka, *Applied Catalysis B: Environmental*, 42 (2003) 13.
- [100] M. Kositzki, A. Antoniadis, I. Poulios, I. Kiridis and S. Malato, *Solar Energy*, 77 (2004) 591.
- [101] M. Kositzki, I. Poulios, S. Malato, J. Cáceres and A. Campos, *Water Res.*, 38, (2004) 1147.

- [102] M. Hincapié, G. Peñuela, M. I. Maldonado, O. Malato, P. Fernández, I. Oller, W. Gernjak, and S. Malato, *Appl. Catal B: Environ*, 64 (2006) 272.
- [103] European Commission, Implementation of Council Directive 91/271/EEC of 21 May 1991 concerning urban waste water treatment, as amended by Commission Directive 98/15/EC of 27 February 1998. Commission of the European Communities, COM(2004) 248 final, Brussels, 2004.
- [104] A.R. Fernández-Alba, D. Hernando, A. Agüera, J. Cáceres and S. Malato, *Wat. Res.*, 36 (2002) 4255.
- [105] V. Sarria, S. Parra, N. Adler, P. Péringier, N. Benitez and C. Pulgarin, *Catalysis Today*, 76 (2002) 301.
- [106] S. Parra, C. Pulgarín and S. Malato, *Appl. Catal. B: Environ.*, 36 (2002) 131.
- [107] M. Pratap, B. Srinivas, V. Durga, M. Subrahmanyam and P.N. Sharma, *Toxicol. Environ. Chem.*, 86 (2004) 125.
- [108] Arques, A. García, R. Sanchís, L. Santos-Juanes, A.M. Amat, M.F. López and M.A. Miranda, *J. Solar Energy Engineering*, in press (2006).
- [109] M. Lapertot, C. Pulgarín, P. Fernández, M. I. Maldonado, L. Pérez, I. Oller, W. Gernjak and S. Malato, *Wat Res.*, 40 (2006) 1086.
- [110] Oller, P. Fernández-Ibáñez, M.I. Maldonado, L. Pérez-Estrada, W. Gernjak, C. Pulgarín, P.C. Passarinho and S.Malato, *Res. Chem. Interm.*, in press (2006).
- [111] R. Dillert, S. Vollmer, M. Schober, J. Theurich, D. Bahnemann, H.-J. Arntz, K. Pahlmann and G. Sager, *Chem. Eng. Technol.*, 22 (1999) 931.
- [112] R. Dillert, S. Vollmer, E. Gross, M. Schober, D. Bahnemann, J. Wienefeld, K. Pahlmann, T. Schmedding, H.J. Arntz, and G. Sager, *Z. Phys. Chem.*, 213 (1999) 141.
- [113] H. Freudenhammer, D. Bahnemann, L. Bousselmi, S.U. Geissen, A. Ghrabi, F. Saleh, A. Si-Salah, U. Siemon and A. Vogelpohl, *Wat. Sci. Tech.* 35 (1997) 149.
- [114] S.-U. Geissen, Xi W. Weidemeyer, A. Vogelpohl, A. Bousselmi, L. Ghrabi and A. A. Ennabli, *Water Science and Technology*, 44 (2001) 245.
- [115] J. Blanco, S. Malato, P. Fernández, A. Vidal, A. Morales, P. Trincado, J. C. Oliveira, C. Minero, M. Musci, C. Casalle, M. Brunotte, S. Tratzky, N. Dischinger, K.-H. Funken, C. Sattler, M. Vincent, M. Collares, J. F. Mendes and C.M. Rangel, *Solar Energy*, 67 (2000) 317.
- [116] S. Malato, J. Blanco, A. Vidal, P. Fernández, J. Cáceres, P. Trincado, J. C. Oliveira and M. Vincent, *Chemosphere*, 47 (2002) 235.
- [117] P. Fernández-Ibáñez, J. Blanco, S. Malato and F. J. de las Nieves, *Wat. Res.*, 37 (2003) 3180.
- [118] Sattler, L. de Oliveira, M.Tzschirner and A.E.H. Machado, *Energy*, 29 (2004), 835.
- [119] E. H. Machado, J. A. de Miranda, R. F. de Freitas, E. T. Duarte, L. F. Ferreira, Y. D. T. Albuquerque, R. Ruggiero, C. Sattler and L. de Oliveira, *J. Photochem. Photobiol. A: Chem.*, 155 (2003) 231.
- [120] E. H. Machado, T. P. Xavier, D. Rodrigues de Souza, J. A. de Miranda, E. T. F. Mendonça Duarte, R. Ruggiero, L. de Oliveira and C. Sattler, *Solar Energy*, 77 (2004) 583.
- [121] M. Amat, A. Arques, M. A. Miranda and S. Seguí, *Solar Energy*, 77 (2004) 559.

Waste water treatment by advanced oxidation processes (solar photocatalysis in degradation of industrial contaminants). Case Study I: pilot plant studies.

Sixto Malato

Plataforma Solar de Almería-CIEMAT. Carretera Senés km4, Tabernas (Almería).
04200-Spain. Telf. 34- 950387940. Fax. 34-950365015. e-mail: sixto.malato@psa.es

1. INTRODUCTION

Industrial waste water containing toxic and/or non-biodegradable organic pollutants are not treatable by conventional biological processes. Although biological treatment is often the most cost-effective alternative it is often not effective for industrial effluents contaminated with biorecalcitrant organic substances. The high potential and effectiveness of Advanced Oxidation Processes (AOPs) for the total oxidation of hazardous organic compounds is widely recognized [1,2]. AOPs are characterized by the production of hydroxyl radicals ($\bullet\text{OH}$), the second strongest known oxidant after fluorine. This hydroxyl radical attacks organic molecules, yielding carbon dioxide, inorganic ions and water. The advantage of AOPs is enhanced by the fact that $\bullet\text{OH}$ radicals may be produced in different ways, so they can be adapted to specific treatment requirements.

Among the AOPs, the photo-Fenton system [3], has been shown to be the most promising for the remediation of contaminated water [4]. Moreover, as UV radiation generation by lamps or ozone production is expensive, photo-Fenton driven by solar radiation is of special interest, making the development of suitable technologies very attractive for practical applications [5-6]. The major drawback of AOPs is that their operating costs exceed those of biological treatment. Nevertheless, the use of AOPs as a pre-treatment step to enhance the biodegradability of waste water containing recalcitrant or inhibitory pollutants can be justified if the resulting intermediates are easily degradable by micro-organisms in further biological treatment. Many reports have focused on the study of new chemical-oxidation technologies as a pre-treatment for non-biodegradable or toxic waste water combined with a conventional biological treatment [7-9]. These results, mainly from laboratory studies, suggest potential advantages for water treatment. Recently, very attractive combined systems have been proposed to treat different kinds of industrial waste water [10-16]. Today combined photo-assisted AOP and biological processes are gaining in importance as treatment systems, as one of the main urban waste water treatment obligations imposed by European Union Council Directive 91/271/EEC is that waste water collecting and treatment systems (generally involving biological treatment), must be in place in all agglomerations of between 2000 and 10000 population equivalents by 31st December 2005. Smaller agglomerations which already have a collecting system must also have an appropriate treatment system by the same date [17]. In a near future, AOP plants developed in the EU could be discharging pre-treated waste water into a nearby conventional biological treatment plant.

This work evaluates the feasibility of coupling a photoreactor with to a biological field system at pilot scale employing photo-Fenton pre-treatment of a biorecalcitrant industrial compound, α -methylphenylglycine (MPG), dissolved in distilled water and simulated seawater. This two extreme situations are compared, as the photo-Fenton reaction rate in waste water containing typical freshwater inorganic species (in the range of mM units), is usually almost the same as in demineralised water. It should be

remarked that a pH between 2.8-2.9 (optimal for photo-Fenton treatment) avoids the presence of inorganic carbon species, which are purged as CO₂ during pH adjustment of the waste water. A different situation arises in the presence of large quantities of sodium chloride (i.e., seawater), when photo-Fenton very often is not able to substantially mineralise the organic content of the waste water [18, 19]. MPG, a common precursor in pharmaceuticals, was selected because of its non-biodegradability and high water solubility. Degradation and mineralization (TOC disappearance) of the parent compound were analysed, and nitrification and denitrification phenomena were also observed. Experiments in chemical and biological characterisation of phototreated solutions were performed in order to establish when the phototreated solution becomes biocompatible. The biological system (immobilised biomass reactor) which completes the photochemical pre-treatment should be compact, modular, flexible and resistant to toxic shock, and variations in charge and flow.

2. EXPERIMENTAL

2.1. Chemicals

Technical-grade MPG (α -methylphenilglycine, C₉H₁₁NO₂) was used as received (Diagram 1). The initial concentration in all experiments was 530 mg L⁻¹. MPG tests were performed using distilled water from the Plataforma Solar de Almería (PSA) distillation plant (conductivity < 10 μ S cm⁻¹, Cl⁻ = 0.7-0.8 mg L⁻¹, NO₃⁻ = 0.5 mg L⁻¹, organic carbon < 0.5 mg L⁻¹), and simulated seawater prepared with 35 g L⁻¹ of NaCl (reagent grade, Panreac). Photo-Fenton experiments were performed using iron sulphate (FeSO₄.7H₂O), reagent grade hydrogen peroxide (30% w/v) and sulphuric acid for pH adjustment (around 2.7-2.9), all provided by Panreac. The phototreated solutions were neutralized by means of NaOH (reagent grade, Panreac). Neutral pH of the solutions was maintained during the biological treatment by adjusting with H₂SO₄ (reagent grade, Panreac) and NaOH. The nutrient salts used in the biological reactor (P, N, K and oligoelements) were added from standard solutions (Panreac).

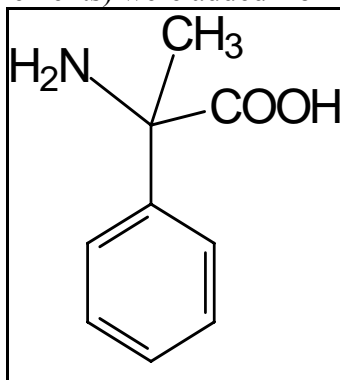


Diagram 1. Chemical structure of α -methylphenilglycine (MPG).

2.2. Analytical determinations

MPG concentration was analysed using reverse-phase liquid chromatography (flow 0.5 ml.min⁻¹) with a UV detector in an HPLC-UV (Agilent Technologies, series 1100) with C-18 column (LUNA 5 μ m, 3mm x 150 mm from Phenomenex). Ultra pure distilled-deionised water obtained from a Milli-Q (Millipore Co.) system and HPLC-graded organic solvents were used to prepare all the solutions. The mobile phase composition employed for detecting the pollutant was phosphoric acid at 50 mM adjusted to pH 2.5 with NaOH, at a wavelength of 210 nm. Mineralization was monitored by measuring the Total Organic Carbon (TOC) by direct injection of filtered samples into a Shimadzu-5050A TOC analyser provided with a NDIR

detector and calibrated with standard solutions of potassium phthalate. Ammonium concentration was determined with a Dionex DX-120 ion chromatograph equipped with a Dionex Ionpac CS12A 4mm x 250 mm column. Isocratic elution was done with H₂SO₄ (10 mM) at a flow rate of 1.2 mL min⁻¹. NH₄⁺ was measured in simulated saline samples using the Colorimetric Phenate Method (American Standard Methods, n° 4500). Anion concentrations (NO₃⁻ and NO₂⁻) were determined with a Dionex DX-600 ion chromatograph using a Dionex Ionpac AS11-HC 4mm x 250 mm column. The gradient programme was pre-run for 5 min with 20 mM NaOH, an 8-min injection of 20 mM of NaOH, and 7-min with 35 mM of NaOH, at a flow rate of 1.5 mL min⁻¹. Colorimetric determination of total iron concentration with 1,10-phenantroline was used following ISO 6332. Hydrogen peroxide analysis was carried out by iodometric titration, although, since this method is very time consuming (around 45 minutes), it was frequently determined in fresh sample solutions using Merckoquant Paper (Merck Cat. No. 1.10011.0001) just to get an idea of overall H₂O₂ consumption and to detect any significant decrease.

2.3. Biodegradability assays

An adaptation of the EC protocol (Directive 88/303/EEC) was followed to determine the biocompatibility of the pre-treated MPG waste water at different stages of photo-Fenton process. This method, called the Zahn-Wellens test (Z-W), is used to evaluate the biodegradability of water-soluble, non volatile organic contaminants when exposed to relatively high concentrations of micro-organisms. Activated sludge from the Waste water Treatment Plant in Almería (AQUALIA), mineral nutrients and test material as the sole carbon source are placed together in a 0.25-L glass vessel equipped with an agitator and aerator. The test lasts around 28 days and is kept at 20-25°C under diffuse illumination (or in a dark room). The blank is prepared using distilled water instead of test water, mineral nutrients and an amount of bacteria representative of the inoculum present in the test solutions. A vessel containing diethylene glycol, a well-known biodegradable substance recommended by the protocol mentioned above is run in parallel in order to check the activity of the activated sludge. Degradation is monitored by DOC determination in the filtered solution (with the TOC analyser), daily or at other appropriate regular time intervals. The initial DOC is always determined three hours after test start-up in order to detect adsorption of contaminants by the activated sludge. Loss of volume from evaporation (due to agitation and aeration) is adjusted before each sampling with distilled water in the required amounts. The ratio of eliminated DOC after each interval to the initial DOC is expressed as the percentage of biodegradability: $100 [1 - (C_t - C_B / C_A - C_{BA})]$. C_A is the DOC (mg/L) in the test mixture, measured three hours after the beginning of the test, C_t is the DOC at time t, C_B is the DOC of the blank at time t and C_{BA} is the DOC of the blank three hours after the beginning of the test. The results are plotted against time giving the percentage of biodegradation. Samples analysed are considered biodegradable when the biodegradation percentage is over 70% [20].

2.4. Experiment set-up

2.4.1. Photoreactor

Photo-Fenton experiments were carried out under sunlight in a pilot plant specially developed for photo-Fenton applications installed at Plataforma Solar de Almería (PSA, Almería, Spain). This solar reactor is composed of a continuously stirred

tank, a centrifugal pump (1.5 m³ h⁻¹), a solar collector and connecting tubing and valves. The total reactor volume of 75 L is composed of two parts: 44.6 L (glass tubes) corresponding to the total irradiated volume (V_i), and the dead reactor volume (tank + tubes). The solar collector is made up of four Compound Parabolic Collector units (1.04 m² each one), mounted on an aluminium frame fixed on a south-facing platform tilted at the local latitude (37°). Each collector unit is provided by five 50 mm outer diameter borosilicate-glass tubes connected by plastic joints. A flow diagram is shown in figure 1. The pilot plant is outdoors, but a temperature control system keeps the temperature at a set point of 30°C. Details of the pilot plant have been published elsewhere [21]. Solar ultraviolet radiation (UV) was measured by a global UV radiometer (KIPP&ZONEN, model CUV 3), mounted on a platform tilted 37°, which provides data in terms of incident W_{UV}.m⁻². In this way, the energy reaching any surface is measured in the same position with regard to the sun. With equation 1, combination of the data from several days' experiments and their comparison with other photocatalytic experiments is possible.

$$t_{30W,n} = t_{30W,n-1} + \Delta t_n \frac{UV}{30} \frac{V_i}{V_T}; \quad \Delta t_n = t_n - t_{n-1} \quad (1)$$

Where t_n is the experimental time for each sample, UV is the average solar ultraviolet radiation measured during Δt_n, and t_{30W} is a “normalized illumination time”. In this case, time refers to a constant solar UV power of 30 W.m⁻² (typical solar UV power on a perfectly sunny day around noon).

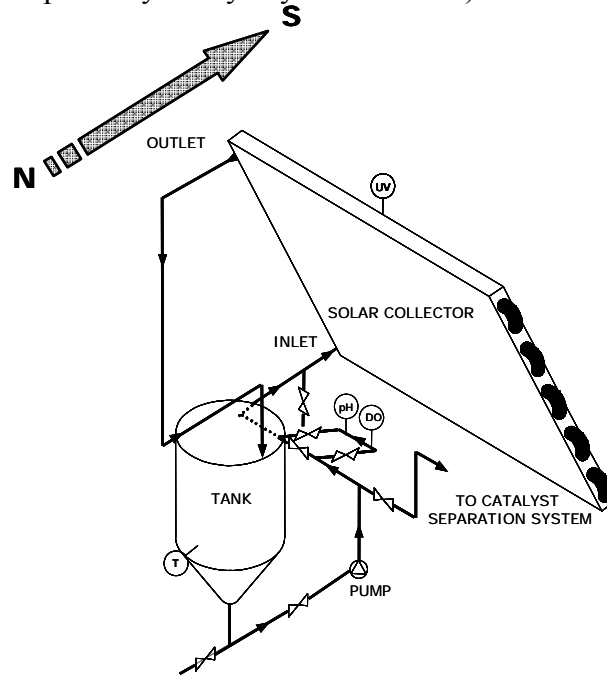


Figure 1. Flow diagram of the photoreactor (photo-Fenton).

At the beginning of all the photo-Fenton experiments, with the collectors covered and the reactor filled with distilled water, MPG was directly added to the photoreactor, and a sample was taken after 15 minutes of homogenisation (initial concentration). In the case of experiments with simulated seawater, 35 g L⁻¹ of NaCl was added and homogenized well before adding MPG. Then the pH was adjusted between 2.8-2.9 with sulphuric acid in order to avoid iron hydroxide precipitation and another sample was taken after 15 minutes to confirm the pH. Afterwards, iron salt was also added (FeSO₄.7H₂O, 2 mg L⁻¹ or 20 mg.L⁻¹ of Fe²⁺, Point 1) and

homogenised well for 15 minutes before a sample was taken. Finally an initial dose of hydrogen peroxide was added (100 ml, Point 2) and different samples were taken to evaluate any effect in the dark, mainly the Fenton process. At that moment collectors were uncovered and photo-Fenton began. The concentration of peroxide in the reactor had to be kept in the range of 200-500 mg L⁻¹ throughout the process, so hydrogen peroxide was frequently analysed off-line and manually controlled to avoid complete disappearance by adding small amounts as consumed.

2.4.2. Biological reactor system

The biological reactor erected for combined-system experiments at the PSA is composed of three modules: a 165-L conic neutralisation tank, a 100 L conic conditioner tank and a 170 L aerobic Immobilised Biomass Reactor (IBR). A flow diagram of the pilot system is shown in figure 2. The conditioner tank is equipped with a pH control unit (CRISON, electrode and pH28 controller) for pH adjustment using either H₂SO₄ or NaOH dosed by means of two peristaltic pumps (ALLDOS). The IBR is a flat bottom container filled with 90-95 L of propylene Pall® Ring supports (nominal diameter: 15 mm, density: 80 kg m⁻³, specific area: 350 m² m⁻³, void fraction: 0.9 m³ m⁻³), colonized by activated sludge from the municipal waste water treatment plant in Almería. This bioreactor is also equipped with an air blower to supply oxygen to the micro-organisms, and a dissolved oxygen (DO) control unit (CRISON, electrode and OXI49 controller) for maintaining oxygen in the system between 4 mg L⁻¹ to 6 mg L⁻¹. All the experiments performed in this biological system were carried out in batch mode operation. MPG waste water pre-treated by photo-Fenton was pumped into the neutralisation tank, where pH was neutralised by NaOH to a pH around 7. This favoured catalyst (Fe²⁺) settling and separation when necessary. Following this preliminary step, the photo-pretreated effluent was piped to the conditioner tank by means of a centrifugal pump, where the pH was lightly controlled in a range of 6.5-7.5. Afterwards, the effluent was pumped through the IBR which operated as an up-flow reactor, at a recirculation flow rate of 8 L min⁻¹ between the conditioner tank and the IBR, until the decreased in TOC reached characteristic biological system values (20-30 mg L⁻¹). At that moment combined system treatment of the effluent could be considered complete.

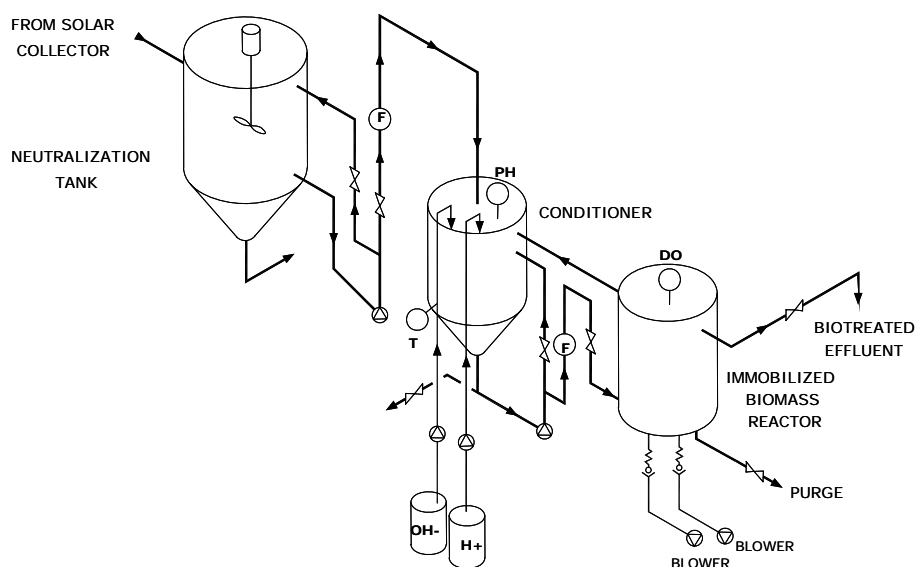


Figure 2. Flow diagram of the biological reactor system.

3. RESULTS AND DISCUSSION

Photodegradation of MPG dissolved in distilled water was evaluated by two photo-Fenton experiments performed with two different catalyst concentrations, 2 mg L⁻¹ and 20 mg L⁻¹ of Fe²⁺. Their comparison made it possible to select optimal photocatalytic conditions for testing the integrated system. It is worth mentioning that heterogeneous photocatalysis with TiO₂ has been demonstrated, as reported in previous publications, to be less efficient than homogeneous photocatalysis by photo-Fenton for treating this type of waste water [21]. On the other hand, photo-Fenton at 20 mg L⁻¹ of Fe²⁺ has previously been found optimum for the specially designed solar photoreactor used in this work, not only from the point of view of degrading specific contaminants [22], but also from the point of view of the solar photoreactor optical behaviour [23]. In any case, as the purpose of our work was to evaluate the feasibility of integrating a photoreactor and a biological system, photo-Fenton also was tested with only 2 mg L⁻¹ of Fe²⁺ to determine whether waste water biocompatibility could be reached in a reasonable length of time, as low iron concentrations are enough for the photocatalytic pre-treatment step. All the experiments were carried out at the same MPG concentration of around 530 mg L⁻¹. All the experiments were performed at the same initial concentration of MPG, selected because the main purpose of the work was to assess whether it was possible to achieve biodegradability by photo-Fenton. This means converting MPG (known to be non-biodegradable) into other biodegradable organic compounds. As clearly shown in the results, when MPG has disappeared, considerable mineralisation has been attained. Under these circumstances, it was necessary to perform tests at a high enough initial concentration for the Z-W test, as Directive 88/302/EEC recommends testing at 400 mg/L > TOC > 50 mg/L to evaluate properly the biodegradability. The mass balance of the treatment of this compound by photo-Fenton process is based on equation 4, where the combination of the mineralization reaction (equation 2) and the decomposition of hydrogen peroxide (equation 3) are considered:

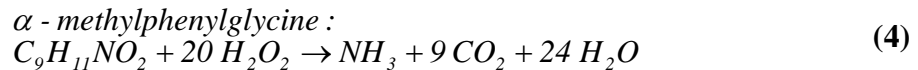
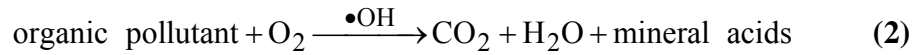


Figure 3 a, shows the degradation and mineralization of MPG during both photo-Fenton processes, as well as the hydrogen peroxide consumption corresponding to each test. It can be observed that when 20 mg L⁻¹ of Fe²⁺ was employed, mineralization was almost complete (97% decrease in TOC), while using a smaller amount of catalyst (2 mg L⁻¹), the treatment time necessary for the same mineralization percentage appeared to be several times longer. Furthermore, the significant compound degradation attained during “dark Fenton” (with the collectors covered, from point 2 to t_{30w} = 0), in both photo-Fenton tests, although it was much more pronounced with the higher catalyst concentration (20 mg L⁻¹) is worthy of mention.

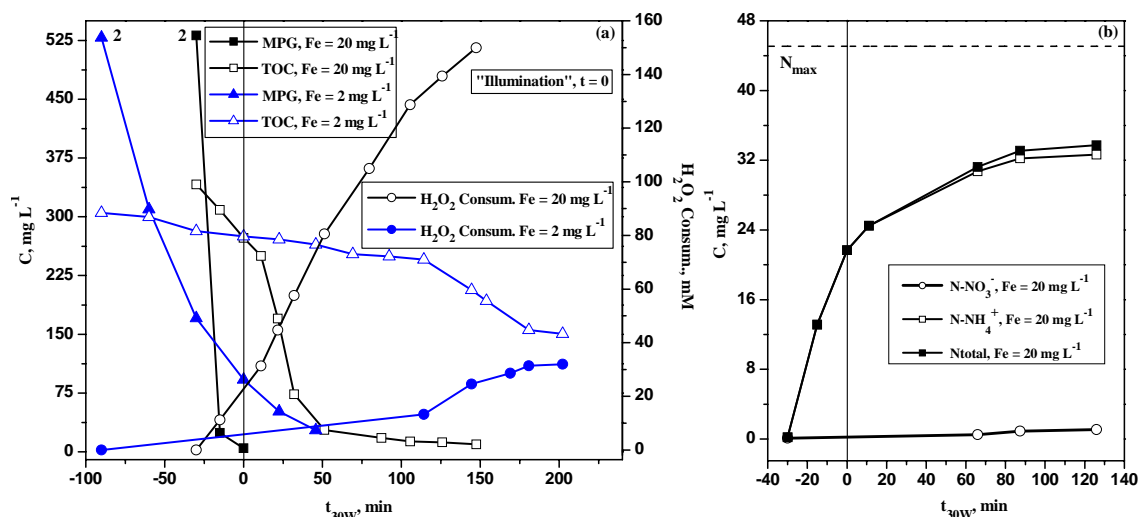


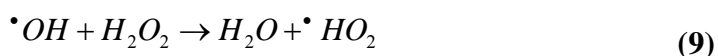
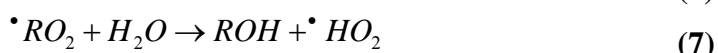
Figure 3 (a). MPG degradation and mineralization by photo-Fenton at 2 mg L^{-1} and 20 mg L^{-1} of Fe^{2+} with distilled water. Point 2 refers to the first addition of H_2O_2 (see subsection “experiment set-up” for details). **(b)** Inorganic ions released during photo-Fenton at 20 mg L^{-1} of Fe^{2+} .

Kinetic studies of these two photo-Fenton processes were performed to support these results. Assuming that the reaction between the $\bullet\text{OH}$ radicals and the pollutant is the rate-determining step, MPG degradation may be described as a first-order reaction (equation 5):

$$r = k_{OH} [\bullet\text{OH}]C = k_{ap}C \quad (5)$$

Where C is the MPG concentration, k_{OH} is the reaction rate constant and k_{ap} is a pseudo first order constant. This was confirmed by the linear behaviour of $\ln(C_0/C)$ as a function of t_{30w} , for both tests performed (see table 1). An appreciable difference between photo-Fenton experiments performed at the two iron concentrations (around eight times faster with 20 mg L^{-1} of Fe^{2+}), was clearly observed (see table 1) not only with regard to the required treatment time, but also to the kinetics rate constant (k_{ap}), and initial reaction rate (r_0). However, at the beginning of the process TOC mineralization was slow until at $t_{30w} = 20 \text{ min}$ (for $\text{Fe}^{2+} = 20 \text{ mg L}^{-1}$) and $t_{30w} = 115 \text{ min}$ (for $\text{Fe}^{2+} = 2 \text{ mg L}^{-1}$), when mineralization rate increased considerably. This effect could be explained by the partial MPG oxidation at the beginning of both treatments and the later complete oxidation of the intermediates generated to CO_2 , and/or the formation of more efficient iron-carboxylic complexes (hydrogen peroxide consumption was also accelerated at those points), as described below.

Hydrogen peroxide consumption was very similar (around 40 mM) for both photo-treatments until 50% of the initial TOC was eliminated (i.e. $\text{TOC} \approx 175 \text{ mg/L}$). These experiments were performed with an excess of H_2O_2 , so the drawback of the hydrogen peroxide self-decomposition reaction must be taken into consideration (equation 3). The incorporation of the dissolved oxygen (from atmosphere and hydrogen peroxide decomposition) in the reaction mechanism by equations 6 and 7 produces a peroxy radical, which can then further participate in the reaction mechanism, generating an additional hydrogen peroxide molecule (equation 8). When MPG degradation proceeds, the ratio of hydrogen peroxide to pollutant increased and the reaction of the radicals generated with hydrogen peroxide (equation 9) were favoured, leading to the much less reactive $\bullet\text{HO}_2$ [30]:



MPG	$t_{30w,50}^{(1)}$ min	k_{ap} min^{-1}	R^2	$r_0^{(2)}$ $\text{mg.L}^{-1}.\text{min}^{-1}$	$H_2O_2\text{CONS}^{(3)}$ mM
Fe = 2 mg L⁻¹	202	0.019	0.999	10.26	32
Fe = 20 mg L⁻¹	22	0.158	0.971	84.01	45

⁽¹⁾ Treatment time necessary to eliminate approximately 50% of initial TOC. ⁽²⁾ Initial degradation rate from the beginning of the process to $t_{30w} = 0$ min ($t_{total} = 30$ min for 20 mg L⁻¹ and $t_{total} = 90$ min for 2 mg L⁻¹). ⁽³⁾ Amount of hydrogen peroxide consumed to eliminate approximately 50% of initial TOC.

Table 1. Kinetic parameters and consumption of hydrogen peroxide to eliminate approximately 50% of initial TOC.

Depending on the ligands, the ferric iron complex has different light adsorption properties and reactions have different quantum yields at different wavelengths. Consequently, pH plays a crucial role in the efficiency of the photo-Fenton reaction, because it strongly influences which complexes are formed, this is why the pH of 2.8 was frequently postulated as optimum for photo-Fenton treatment [24, 25]. At this pH, there is still no precipitation, and the dominant iron species in solution is $[\text{Fe}(\text{OH})]^{2+}$, which is the most photoactive ferric iron-water complex [26]. In fact, ferric iron can form complexes with many substances and undergo photoreduction. Of special importance are carboxylic acids because they are frequent intermediates during the last stages of an oxidative treatment. Such ferric iron-carboxylate complexes can have much higher quantum yields than ferric iron-water complexes. Therefore the reaction typically shows an initial lag phase, until intermediates which can regenerate ferrous iron more efficiently are formed, accelerating the process.

Because of the low solubility of ferric iron hydroxide ($K_s \approx 10^{-37}$), precipitation starts at pH 2.5-3.5, depending on the iron concentration and temperature. The precipitation process starts with the formation of dimers and oligomers, which then gradually further polymerise, and lose water until finally forming insoluble iron hydroxides (e.g. goethite or hematite). This ageing process is slow [27, 28], but precipitation and ageing processes are also temperature dependent. Higher temperatures yield to faster and higher precipitation of the monomer content [29] (no significant change detected during 1 day at 4°C but a decrease of the 4% was observed at 28°C). The tests reported here were performed at higher temperatures (30°C) than those described by Krýsová et al., [29], and therefore, most of the initial Fe^{2+} (2 mg L⁻¹) may have been lost after 2-3 hours of photo-treatment. Ammonium and nitrate ions release from the initial MPG molecule were measured in different relative concentrations during the photo-Fenton ($\text{Fe}^{2+} = 20$ mg L⁻¹) experiment, (figure 3 b). N_{total} is the combination of total nitrogen released as ammonia and nitrate from MPG degradation, which present a molar ratio of $\text{NH}_4^+/\text{NO}_3^- = 28$ at the end of the process ($t_{30w} = 212$ min). This ratio changed during phototreatment, since at shorter treatment times the organic nitrogen was released as

ammonia and high NH_4^+ concentrations were detected, but afterwards it was slowly transformed into nitrate at the end of the process. However, the nitrogen mass balance was incomplete, as only 77% of the theoretical amount appeared after almost complete mineralisation. Other researchers [31] have found that the fate of nitrogen in photocatalytic systems depends on the initial oxidation state. When present in the -3 state, as in amino groups (the case of MPG), nitrogen spontaneously evolves as NH_4^+ cations with the same oxidation state (equations 10 and 11), before being slowly oxidized into nitrate. This is exactly what was observed in the photo-Fenton treatment of MPG.



From these tests, it can be concluded that photo-Fenton treatment appears to be much more effective with 20 mg L^{-1} of Fe^{2+} than with only 2 mg L^{-1} , especially when the organic charge of the waste water was in the range of hundreds of mg L^{-1} , making photo-Fenton treatment times longer. For coupling with biological treatment, it would not be necessary to settle and separate the catalyst, since a concentration of 20 mg L^{-1} is still low enough to ensure non-inhibitory effects. The main purpose of this work was to find out whether it was possible to enhance MPG biodegradability by an oxidative photo-Fenton pre-treatment for disposal in an aerobic biological process. Therefore, taking previous studies into account [12], different stages of photo-Fenton treatment were selected as a reference for evaluating waste water biocompatibility. In figure 4 a, degradation and mineralization of MPG by photo-Fenton (at 20 mg L^{-1} of Fe^{2+}), is shown against treatment time. In this case an H_2O_2 limiting concentration (around 100 mg L^{-1}) was maintained during the whole process to minimize hydrogen peroxide consumption and for optimal Z-W biodegradability analysis conditions (little H_2O_2 to avoid toxic effect). While the theoretical hydrogen peroxide consumption for complete degradation of 530 mg L^{-1} of MPG (as calculated by equation 4) is 64 mM , the one obtained by minimizing hydrogen peroxide consumption during the photo-Fenton treatment was lower (58 mM), this would mean a significant reduction in the corresponding operating costs. Concerning the biocompatibility analysis, a Z-W test was performed taking four pre-treated samples (marked in figure 4 a), just after complete disappearance of MPG. These results are evaluated below.

MPG is also known to be present in industrial saline waste water, so it was considered of interest to test MPG degradation by photo-Fenton (at 20 mg L^{-1} of Fe^{2+} , minimizing H_2O_2 consumption), in simulated seawater prepared by the addition of 35 g L^{-1} of NaCl . Therefore, two experiments with manually controlled addition of hydrogen peroxide were performed, both in distilled water and in simulated seawater using 20 mg L^{-1} of catalyst (figure 4 a). As observed in figure 4 a, the pollutant was also successfully degraded and mineralised (around 90% of TOC disappeared), but this time, the treatment time required for substantial mineralization of MPG was three times longer than in the previous experiment (see Figure 3) performed with distilled water. Table 2 shows a direct comparison between the two photo-Fenton processes (at 20 mg L^{-1} of Fe^{2+}), in distilled water and simulated seawater with an H_2O_2 -limiting concentration. Kinetic studies show a similar first-order kinetic constant (k_{ap}) and initial degradation rate (r_0) in both cases, which means that no significant negative effect was found in the photo-Fenton treatment of MPG due to the characteristics of saline water. Nevertheless, an important drawback related to the treatment time was detected when simulated

seawater was employed. The treatment time necessary for 90 % mineralization was around 3 times higher than for distilled water, leading to higher consumption of hydrogen peroxide. The effect of chloride on Fenton and photo-Fenton processes was recently reported in detail by De Laat et al. [32].

MPG	$t_{30w,90}^{(1)}$ min	k_{ap} min^{-1}	R^2	$r_0^{(2)}$ $\text{mg.L}^{-1}.\text{min}^{-1}$	$\text{H}_2\text{O}_2\text{CONS}^{(3)}$ mM
Fe = 20 mg L⁻¹	121	0.219	0.939	112.83	58
Fe = 20 mg L⁻¹ + 35 g L⁻¹ NaCl	385	0.176	0.959	94.74	154

⁽¹⁾ Treatment time necessary to eliminate approximately 90% of initial TOC. ⁽²⁾ Initial degradation rate from the beginning of the process to $t_{30w} = 0$ for 20 mg L⁻¹ + NaCl ($t_{\text{total}} = 60$ min) and to $t_{30w} = 4.2$ min for 20 mg L⁻¹ ($t_{\text{total}} = t$ min).

⁽³⁾ Amount of hydrogen peroxide consumed to eliminate approximately 90% of initial TOC.

Table 2. Kinetic parameters and consumption of hydrogen peroxide to eliminate 90% of the initial TOC, when MPG was dissolved in distilled water and in simulated seawater

Figure 4 b, shows the percentage of biodegradability in each sample selected for the Z-W test. First of all, the pH of the samples had to be adjusted to 6.5-7.5 (optimal pH for biological systems) with NaOH, as the pH in the photo-Fenton process was around 2.8-2.9. Then, the Z-W was started and maintained properly aerated and agitated for 28 days. As observed in the figure, the percentage of biodegradability in waste water with the higher TOC (163.1 mg L⁻¹ and 124 mg L⁻¹) pre-treated by photo-Fenton was only between 40-50%. Degradation was more pronounced in the first 5 days of biotreatment, but afterwards, no appreciable change was detected. The generation of non-biodegradable (but non-toxic) intermediates during advanced stages of the photo-Fenton treatment could be inferred from these low percentages. Biodegradability over 70% was reached in the samples with lower TOC values in both cases. Biodegradability reached 80% in the sample with TOC = 46.9 mg L⁻¹ in only 2 days and continued increasing until complete biodegradation of TOC. After reaching the maximum, it decreased because of the cell's death (no feed was available) and organic carbon was released from the inside of the cells. On the other hand, the sample with TOC = 92.7 mg L⁻¹, reached only 70% biodegradability in around 5 days and remained the same for the rest of the Z-W test. Samples with a biodegradability of 70% are already considered biodegradable, so the best point for discharging the photo-Fenton effluent to an aerobic biological system could be established as just when MPG was completely degraded and the TOC decreased to around 90-95 mg L⁻¹.

In this sense, the integrated system was better for total mineralization of the photo-treated solution, since using the photo-Fenton reactor alone is not economically attractive for reaching satisfactory mineralization levels. For example, an increase of the operating costs (mainly as hydrogen peroxide consumption) of approximately 20% could be considered when photo-Fenton reactor is used alone. Moreover, the general investment increase (m² of collectors field needed for total mineralization), could be estimated in approximately 50%.

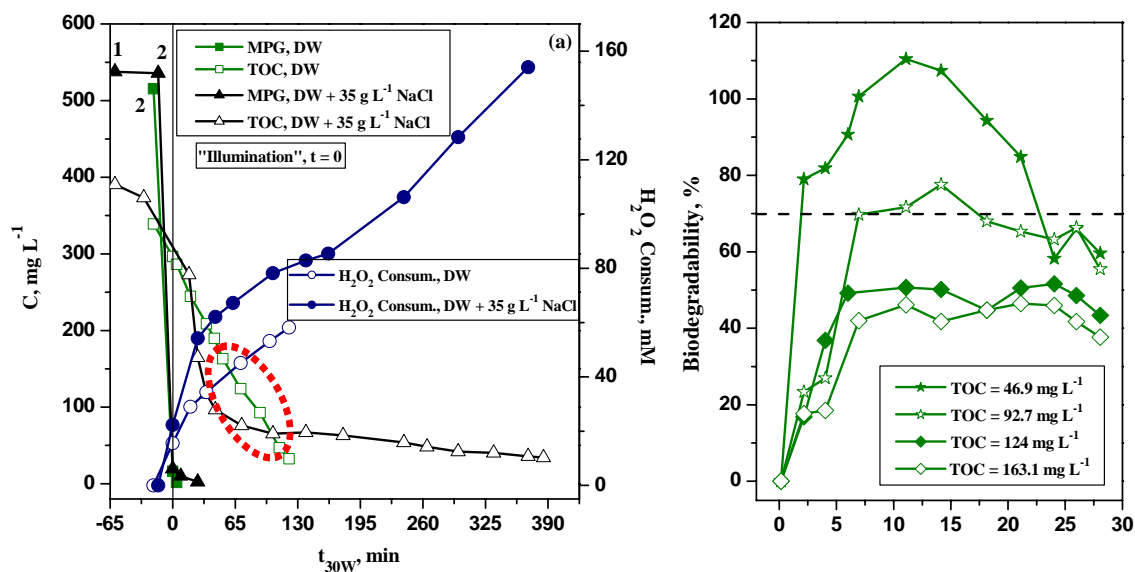


Figure 4. (a) MPG degradation and mineralization by photo-Fenton ($\text{Fe} = 20 \text{ mg L}^{-1}$), with limited additions of H_2O_2 . Point 1 refers to the addition of the catalyst and point 2 to the first addition of H_2O_2 (see subsection “experiment set-up” for details). The surrounded part corresponds to the four samples selected for Z-W. (b) Zahn-Wellens test applied to the samples marked in figure 4 (a).

Taking into account previous similar studies [12,13] and the results above, several batch photo-Fenton experiments were performed (at 20 mg L^{-1} of Fe^{2+}) until complete degradation of MPG and a corresponding TOC of around 95 mg L^{-1} , to provide enough photo-treated water to the biological reactor. First of all, the Immobilised Biomass Reactor was inoculated with 150 L of activated sludge from a municipal waste water treatment plant, and recirculated between the conditioner tank and the IBR for nearly two weeks in order to ensure optimal fixation of the sludge on the polypropylene supports. The total suspended solids, TOC and inorganic ions concentration (mainly ammonia and nitrate) were measured daily.

The analysis of total suspended solids (TSS) was used to assess bacteria fixation on the supports during IBR inoculation, a variation from 0.42 g L^{-1} to 0 in approximately 10 days was detected. That is when the IBR could be considered in adequate condition for the biological treatment of waste water from the photo-Fenton pre-oxidation process. Afterwards, the solution pre-treated with photo-Fenton flowed directly into the neutralisation tank of the biological system and following the procedure explained in the subsection on “experiment set-up” (biological reactor system), the pH was adjusted roughly to 7. Only a few grams per batch of iron sludge were produced because of the low concentration of iron. Then the effluent was pumped to the conditioner tank, where pH was kept between 6.5-7.5, and dissolved oxygen between 4 mg L^{-1} and 6 mg L^{-1} . The mineral medium specified in the Z-W test protocol to ensure proper metabolic activity of the bacteria, was also added considering the ammonia concentration already present in the photo-treated effluent. The biological system was operated in batch mode and recirculated between the conditioner tank and the IBR until the solution TOC remained constant from around 20 mg L^{-1} to 30 mg L^{-1} , which characteristically correspond to background noise from the physiological bacteria activity found in

conventional biological media. Total mineralization was therefore impossible (TOC below 20 mg L⁻¹) in this biological degradation system.

Figure 5 shows the evolution of TOC in both photochemical and biological treatments. It may be observed that the solar system was able to remove 76% of the TOC from an initial load of 430 mg L⁻¹ after 3.5 hours of photo-oxidation. Then the pre-treated solution was discharged to the biological process where complete mineralization was achieved in around 3 days, indicating that the photo-pretreatment was able to produce a biocompatible solution. The global efficiency of this combined system was 95% removal of the initial TOC. Figure 5 also shows the TOC from MPG only. This was calculated by taking the MPG concentration measured by HPLC and transforming it into TOC values. Total elimination of the pollutant before the pre-treated effluent was discharged to the biological system was clearly demonstrated.

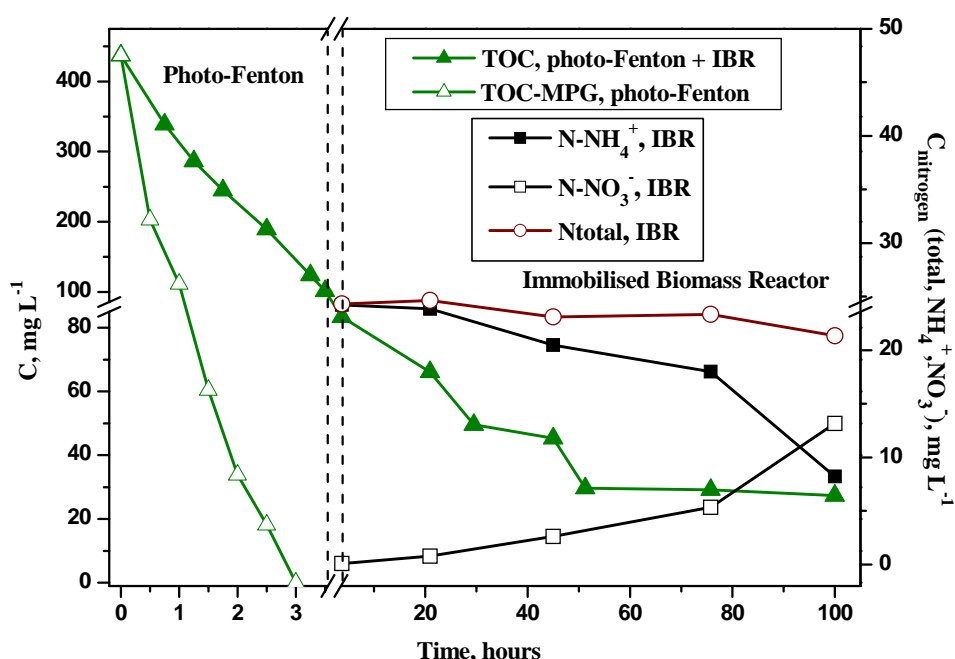
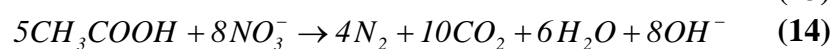
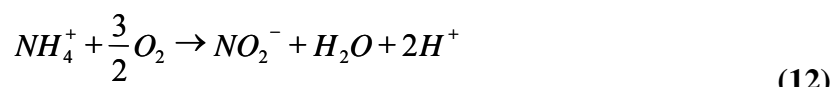


Figure 5. MPG degradation and mineralization by the combined system. Inorganic ions measured in the immobilised biomass reactor are also shown.

Ammonia and nitrate concentrations were also measured during the biological process and plotted against treatment time (see figure 5). As it may be observed, nitrification was detected during biotreatment (equations 12 and 13), meaning that nitrification bacteria consumed the nitrogen from NH₄⁺ for its metabolic activity, and transformed it into NO₃⁻, which was excreted to the media. A decrease in nitrogen concentration from NH₄⁺ of around 16.0 mg L⁻¹ (corresponding to 20.6 mg L⁻¹ of ammonium), was measured, while the nitrogen concentration from NO₃⁻, increased to around 13.1 mg L⁻¹ (57.9 mg L⁻¹ of nitrate). Nevertheless, this increase was lower than expected if all the nitrogen from ammonia had been transformed into nitrate. According to these results, there seemed to be slight denitrification in the last step of the biological process leading to disappearance of around 2.94 mg L⁻¹ of total nitrogen as N₂, and also because of an uptake by bacteria for their growth. This slight elimination of nitrogen occurred because fixed biomass systems have a dissolved oxygen deficiency in the inner wall of the biofilm fixed on the supports, due to the extremely low oxygen transfer to the inner layers of biomass. These anoxic conditions made nitrate became an electron acceptor

(instead of oxygen) for organic carbon oxidation leading to N₂ generation, which was eliminated into the atmosphere (equation 14, where HOAc corresponds to a carbon source, for example acetate).



Denitrification only appeared at the end of the biotreatment as older biomass is required for this process. On the other hand, slight denitrification was detected in the bioreactor due to the low organic carbon source (electron donors) remaining at the end of the biological process.

4. CONCLUSIONS

It has been demonstrated that MPG dissolved in distilled water can be treated successfully by photo-Fenton in a reasonable length of time. Moreover, Photo-Fenton treatment with 20 mg L⁻¹ of Fe²⁺ was efficient enough, and no catalyst separation was required in the combined system, as the concentration was low enough to ensure non-inhibitory effects on the activated sludge. Photo-Fenton (at 20 mg L⁻¹) in simulated seawater was also found to have been successful, but with longer treatment times than for distilled water.

Evaluation of the combined photocatalytic-biological system developed has demonstrated that in batch mode operation, photo-Fenton pre-treatment completely removed the pollutant (MPG) and enhanced its biodegradability, producing a biocompatible effluent which was completely mineralized by the biological system in an Immobilised Biomass Reactor. The combined system was able to totally mineralise 95% of initial TOC of over 400 mg L⁻¹.

The beneficial effects of this two-steps field treatment has therefore been confirmed at pilot scale. Photo-Fenton under sunlight using CPC reactors was able to remove the biorecalcitrant compound and produce biocompatible intermediates required for further biological treatment. These results indicate that a combined solar photocatalytic-biological process is an effective approach for the treatment of biorecalcitrant pollutants present in water.

5. REFERENCES

- [1] P.R. Gogate and A.B. Pandit, *Adv. Environ. Res.*, 8 (2004) 501.
- [2] P. R. Gogate and A.B. Pandit, *Adv. Environ. Res.*, 8 (2004) 553.
- [3] A. Safarzadeh-Amiri, J.R. Bolton and S.R. Cater, *J. Adv. Oxid. Technol.*, 1 (1996) 18.
- [4] C. Pulgarín, M. Invernizzi, S. Parra, V. Sarria, R. Polania and P. Péringier, *Catal. Today*, 54 (1999) 341.
- [5] D. Bahnemann, *Sol. Energy*, 77 (2004) 445.
- [6] S. Malato, J. Blanco, A. Vidal and C. Ritcher, *Appl. Catal. B: Environ.*, 37 (2002) 1.
- [7] A. Marco, S. Esplugas and G. Saum, *Wat. Sci. Technol.*, 35 (1997) 321.
- [8] J.P. Scott and D.F. Ollis, *Environ. Progress*, 14 (1995) 88.

- [9] J.P. Scott and D.F. Ollis, *J. Environ. Engineering*, 122 (1996) 1110.
- [10] S. Parra, S. Malato and C. Pulgarín, *Appl. Catal. B: Environ*, 36 (2002) 131.
- [11] M. Rodríguez, V. Sarria, S. Espulgas and C. Pulgarín, *J. Photochem. Photobiol. A: Chem.*, 151 (2002) 129.
- [12] V. Sarria, S. Parra, N. Alder, P. Péringier, N. Benitez and C. Pulgarín, *Catal. Today*, 76 (2002) 301.
- [13] V. Sarria, S. Kenfack, O. Guilled and C. Pulgarín, *J. Photochem. Photobiol. A: Chem.*, 159 (2003) 89.
- [14] V. Sarria, M. Deront, P. Péringier and C. Pulgarín, *Appl. Catal. B: Environ.*, 40 (2003) 231.
- [15] S. Contreras, M. Rodríguez, F. AlMamani, C. Sans and S. Espulgas, *Wat. Res.*, 37 (2003) 3169.
- [16] M. Bressan, L. Liberatone, N.D'Alessandro, L. Tonucci, C. Belli and G. Ranalli, *J. Agric. Food Chem.*, 52 (2004) 1228.
- [17] EC, Implementation of Council Directive 91/27/EEC of 21 May 1991 concerning urban waste water treatment, as amended by Commission Directive 98/15/EC of 27 February 1998, Commission of the European Communities, COM (2004) 248 final. Brussels, 2004.
- [18] R. Maciel, G.L. Sant'Anna, M. Dezotti, *Chemosphere*, 57 (2004) 711.
- [19] J.E.F. Moraes, F.H. Quina, C.A.O. Nascimento, D.N. Silva, O. Chiavone-Filho, *Environ. Sci. Technol.*, 38 (2004) 1183.
- [20] M. Lapertot, C. Pulgarín, *Wat. Res.*, (2006) in press.
- [21] I. Oller, P. Fernández-Ibáñez, M.I. Maldonado, L. Pérez-Estrada, W. Gernjak, C. Pulgarín, P.C. Passarinho, S. Malato, *Res. Chem. Interm.*, (2006) in press.
- [22] M. Hincapié Pérez, G. Peñuela, M.I. Maldonado, P. Fernández-Ibáñez, I. Oller, W. Gernjak and S. Malato, *Appl. Catal. B: Environ.*, (2006) in press.
- [23] S. Malato Rodríguez, J. Blanco Gálvez, M.I. Maldonado Rubio, P. Fernández Ibáñez D. Alarcón Padilla, M. Collares Pereira, J. Farinha Mendes, J. Correia de Oliveira, *Sol. Energy*, 77 (2004) 513.
- [24] A. Safarzadeh-Amiri, J.R. Bolton, S.R. Cater, *J Adv. Oxid. Technol.*, 1 (1996) 18.
- [25] J.J. Pignatello, *Environ. Sci. Technol.*, 26 (1992) 944.
- [26] J.J. Pignatello, E. Oliveros, A. MacKay, *Critical Rev. Environ. Sci. Technol.*, 36 (2006) 1.
- [27] C.M. Jr. Flynn, *Chem. Rev.*, 84 (1984) 31.
- [28] M. Blesa, E. Matijevic, *Adv. Colloid Interface Sci.* 29 (1989) 173.
- [29] H. Krýsová, J. Jirkovský, J. Krýsa, G. Mailhot, M. Bolte, *Appl. Catal. B: Environ.* 40 (2003) 1.
- [30] W. Gernjak, M. Fuerhacker, P. Fernández-Ibáñez, J. Blanco, S. Malato, *Appl. Catal. B: Environ.* 64 (2006) 121.
- [31] H. Lachheb, E. Puzenat, A. Houas, M. Ksibi, E. Elaloui, C. Guillard, J.M. Herrmann, *Appl. Catal B: Environ.*, 39 (2002) 75.
- [32] J. De Laat, G.T. Lee, B. Legube, *Chemosphere*, 455 (2004) 715.

Waste water treatment by advanced oxidation processes (solar photocatalysis in degradation of industrial contaminants). Case Study II: industrial plant.

Sixto Malato

Plataforma Solar de Almería-CIEMAT. Carretera Senés km4, Tabernas (Almería).
04200-Spain. Telf. 34- 950387940. Fax. 34-950365015. e-mail: sixto.malato@psa.es

1. INTRODUCTION

Chemical pollution of surface water can perturb aquatic ecosystems, causing loss of habitats and biodiversity. Humans are exposed to pollution of the aquatic environment by consuming fish or seafood, drinking water and possibly in recreational activities. Pollutants from various sources (e.g. agriculture, industry, incineration) may be released to the environment as products or as unintended by-products, and they may be historical or used daily in household products. In the European Union, water policy is constantly being adapted to protect and improve the quality of Europe's fresh water resources. Article 16 of the Water Framework Directive 2000/60/EC (WFD), for instance, sets out a strategy for dealing with chemical pollution of water.

Although conventional biological treatment is often the most cost-effective alternative, industrial wastewater containing toxic and/or non-biodegradable organic pollutants cannot be treated by biological systems. Therefore, new powerful, clean and safe decontamination technologies must be developed. Among the different treatments available for industrial effluents containing recalcitrant pollutants, Advanced Oxidation Processes (AOPs) have been widely proven to be highly efficient¹⁻⁵. AOPs are characterized by the production of hydroxyl radicals ($\bullet\text{OH}$), which are able to oxidise and mineralise almost any organic molecule, yielding CO_2 and inorganic ions. Due to the reactivity of hydroxyl radicals, their attack is unselective, which is useful for the treatment of wastewater containing many different contaminants⁶. The use of AOPs for wastewater treatment has been studied extensively, but UV radiation generation by lamps or ozone production is still expensive. Therefore, research is focusing on AOPs which can be driven by solar radiation (photo-Fenton and heterogeneous catalysis with UV/ TiO_2), making their development very attractive for practical applications⁷⁻¹⁰. The photo-Fenton process, which combines Fenton (addition of H_2O_2 to Fe^{2+} salts) and UV-Vis light¹¹, has been demonstrated to be the most promising such technology for treating wastewater containing pollutants at concentrations¹²⁻¹⁶ over 10 mg L^{-1} , as the reaction rate is usually much faster than TiO_2 photocatalysis and separation of iron is very often unnecessary¹⁷. The major drawback of AOPs is that their operating costs exceed those of biological treatment. One of the most attractive approaches for process optimisation in this sense is coupling AOPs with a biological treatment¹⁸⁻²⁰. In these integrated systems, AOPs are usually employed as a pre-treatment to enhance the biodegradability of waste water containing recalcitrant or inhibitory pollutants. Recently, very attractive combined systems have been proposed to treat different kinds of industrial wastewater²¹⁻²⁵.

This work evaluates the technical feasibility of pre-industrial combined solar photo-Fenton/aerobic biological treatment of a highly saline industrial wastewater containing around 600 mg L^{-1} of a non-biodegradable compound (α -methylphenylglycine, MPG) and $400\text{-}700 \text{ mg L}^{-1}$ total organic carbon (DOC). The purpose of this treatment strategy was to achieve sufficient biodegradability of the photo-oxidized effluent to allow its discharge into an aerobic Immobilised Biomass Reactor (IBR). Based on results in pilot plant treatment of the non-biodegradable pollutant (MPG) dissolved in distilled water,

model highly saline ($\text{NaCl } 35 \text{ g L}^{-1}$) water¹⁷ and real wastewater²⁶, a new hybrid photocatalytic-biological demonstration plant with a 4-m^3 daily treatment capacity was designed and erected on the grounds of a pharmaceutical company located in the south of Spain²⁷. Pre-industrial-scale results are compared with those found at pilot plant scale (MPG dissolved in real wastewater) and the overall efficiency of the combined treatment is evaluated.

2. MATERIALS AND METHODS

2.1. Chemicals.

Technical-grade α -methylphenylglycine (MPG, $\text{C}_9\text{H}_{11}\text{NO}_2$, 100% purity), a bio-recalcitrant by-product produced during synthesis of pharmaceuticals, was used in this study as received (see MPG chemical structure inserted in Figure 3 (a)) at a concentration of 600 mg L^{-1} ($\text{DOC} = 393 \text{ mg L}^{-1}$) dissolved in the real effluent from an industrial pharmaceutical plant. The composition of this wastewater (without MPG) is typically $\text{NH}_4^+ = 0\text{-}40 \text{ mg L}^{-1}$, $\text{NO}_3^- = 200\text{-}600 \text{ mg L}^{-1}$, $\text{COD} = 40\text{-}400 \text{ mg L}^{-1}$, $\text{DOC} = 20\text{-}200 \text{ mg L}^{-1}$, suspended solids = $20\text{-}100 \text{ mg L}^{-1}$ in seawater $\text{Cl} = 19 \text{ g L}^{-1}$, $\text{SO}_4^{2-} = 2.7 \text{ g L}^{-1}$, $\text{Na} = 11 \text{ g L}^{-1}$, $\text{Mg} = 1.3 \text{ g L}^{-1}$, $\text{Ca} = 0.5 \text{ g L}^{-1}$, $\text{K} = 0.4 \text{ g L}^{-1}$, Conductivity = 55 mS . Photo-Fenton experiments were performed using iron sulphate ($\text{FeSO}_4 \cdot 7\text{H}_2\text{O}$, $20 \text{ mg L}^{-1} \text{ Fe}^{2+}$), reagent-grade hydrogen peroxide (30% w/v) and sulphuric acid for pH adjustment (around 2.3-2.5), all provided by Panreac. The pH of the photo-treated solutions was neutralized prior to bio-treatment and maintained during the biological treatment by automatic adjustment with NaOH (reagent grade, Panreac).

2.2 Analytical determinations.

MPG concentration was analysed using reverse-phase liquid chromatography (flow rate 0.5 ml min^{-1}) with a UV detector in an HPLC-UV (Agilent Technologies, series 1100) with C-18 column (LUNA $5 \mu\text{m}$, $3 \text{ mm} \times 150 \text{ mm}$ from Phenomenex). The mobile phase composition employed for detecting the pollutant was phosphoric acid at 50 mM adjusted to pH 2.5 with NaOH, at a wavelength of 210 nm . Mineralization was monitored by measuring dissolved organic carbon (DOC) by direct injection of filtered samples into a Shimadzu-5050A TOC analyser provided with an NDIR detector and calibrated with standard solutions of potassium phthalate. Samples were filtered through $0.22\text{-}\mu\text{m}$ -pore size PTFE syringe-driven filters (Millipore Millex[®] GN). Ammonium, nitrate and nitrite concentrations in the outlet of the biological treatment were measured by Merck kits (ref: 1.14658.0001 for NH_4^+ , ref: 1.14542.0001 for NO_3^- and ref: 1.14657.001 for NO_2^-). Hydrogen peroxide in the photo-Fenton experiments was analysed by iodometric titration.

2.3. Experimental set-up.

The demonstration plant designed and erected for the combined solar photo-Fenton / biological treatment of saline non-biodegradable industrial wastewater is made up of a photo-Fenton plant and an aerobic biological system. It was erected on the grounds of a pharmaceutical company located in the south of Spain (see Figure 1).



Figure 1. Views of the combined solar photo-Fenton /biological demonstration plant. Solar collector field (left), conditioner tank and Immobilised Biomass Reactor (right).

2.3.1. Solar photo-Fenton plant.

The solar photo-Fenton reactor consists of a 3000-L buffer or recirculation tank, a centrifugal pump (A4-stainless steel Grunfos, recirculation flow rate of $11 \text{ m}^3 \text{ h}^{-1}$), and 100-m^2 solar collector field made up of three rows of Compound Parabolic Collectors (CPCs) specially developed for photo-Fenton applications. 15 CPC modules were arranged in each row and 50-mm-diameter glass absorber tubes were mounted on an aluminium frame tilted 37° (see Figure 1 (left)). The total system volume is 4000 L (1260 L of illuminated volume), with three in-line sensors, pH (Sensolyt probe, WTW), dissolved oxygen (Trioximatic 700IQ probe, WTW) and hydrogen peroxide concentration (H_2O_2 Electrode & controller support, ALLDOS, $0\text{-}2000 \text{ mg L}^{-1}$), in the polypropylene piping (see diagram in Figure 2). The pH and oxygen probe insertions in the piping are PVC-C. The buffer tank is a conical-bottomed vessel for settling and removing suspended solids when necessary. Solar ultraviolet radiation (UV) was measured by a global UV radiometer (KIPP&ZONEN, model CUV 3) mounted on a platform with the same tilt as the collectors. The system is completed by an electric and electronic instrument panel in the field and a PC for on-line data acquisition. With Equation 1, combination of the data from several days' experiments and their comparison with other photocatalytic experiments is possible.

$$t_{30W,n} = t_{30W,n-1} + \Delta t_n \frac{UV}{30} \frac{V_i}{V_T}; \quad \Delta t_n = t_n - t_{n-1} \quad (1)$$

Where t_n is the experimental time for each sample, UV is the average solar ultraviolet radiation measured during Δt_n , and t_{30W} is a "normalized illumination time". In this case, time refers to a constant solar UV power of 30 W m^{-2} (typical solar UV power on a perfectly sunny day around noon). Photo-Fenton experiments were carried out by filling the whole plant with saline industrial wastewater (from the pharmaceutical company's wastewater treatment plant), adjusting the pH to 2.3-2.5 (with H_2SO_4), and adding the pre-dissolved non biodegradable MPG until the desired concentration of 600 mg L^{-1} was achieved. Although it is widely known that the optimal pH for photo-Fenton experiments is 2.8-2.9, in this particular case it was reduced to 2.3-2.5 in order to avoid a pH over 2.9 during the treatment, due to MPG nitrogen released as ammonium (see comments in Section 3.1). This mixture was properly homogenized by turbulent recirculation for half an hour. Then the ferrous iron salt was added (20 mg L^{-1} of Fe^{2+}) and after another 30 minutes of homogenisation, the amount of hydrogen peroxide required according to previous pilot plant experiments (16 litres which corresponds to 35 mM), was added²⁶. Hydrogen peroxide was measured frequently and consumed reagent was replaced (6 litres which corresponds to $13 \text{ mM H}_2\text{O}_2$) when around 40% of

initial DOC was mineralised (see Figure 3 (a)). The collectors were always uncovered during homogenisation. Therefore it was not possible to differentiate the quick Fenton reaction at the beginning (when all the iron was as Fe^{2+}) from photo-Fenton. In any case, with such a strong concentration of organics (hundreds of mg L^{-1} of DOC) and such a low concentration of iron, the effect of the Fenton reaction at the beginning was not very relevant. Indeed, the reaction rate was governed mainly by the slower photochemical reactions, as described in Results and Discussion section with regard to Figure 3.

2.3.2. Immobilised activated-sludge biotreatment plant.

The aerobic biological demonstration plant for combined photo-Fenton/Biological experiments consists of three modules, a 5000-L neutralisation tank, a 2000-L conditioner tank and a 1000-L Immobilised Biomass Reactor (IBR) (Figure 1 (right)). All the tanks were made in polypropylene. The IBR is a flat-bottomed vessel filled with 700 L of polypropylene Pall[®] Ring supports (nominal diameter 15 mm, density 80 kg m^{-3} , specific area $350 \text{ m}^2 \text{ m}^{-3}$, void fraction $0.9 \text{ m}^3 \text{ m}^{-3}$), colonized by activated sludge from the wastewater treatment plant installed at the pharmaceutical company itself. This bioreactor is also equipped with two air diffusers supplied with compressed air through independent pipes regulated with ball valves. Each diffuser can supply up to $10 \text{ N m}^3 \text{ h}^{-1}$ of air. On-line pH and dissolved oxygen sensors are also placed in the conditioner tank return pipe. Both are connected to an automatic controller for automatic conditioner tank pH adjustment between 6.8 and 7.5 and dissolved oxygen between 4-6 mg L^{-1} in the IBR by acting on two pneumatic valves that feed air diffusers. The pH probe also has a Pt-100 sensor for monitoring the water outlet temperature (Figure 2).

This biological system was operated directly in continuous mode, because the purpose was to maintain the immobilised activated-sludge reactor working under the real conditions prevailing in a conventional wastewater treatment plant. It was operated in batch mode only during the start-up phase (IBR inoculation, bacteria fixation and growing, etc) (see Section 3.2). The industrial saline wastewater partially oxidized by photo-Fenton was discharged into the neutralisation tank (in Figure 2, valve (1) closed and (2) opened), which is a conical-bottomed vessel where water was roughly neutralised with concentrated NaOH and iron was settled and removed when necessary. Then the photo-pre-treated effluent was transferred to the conditioner tank, where the pH was automatically adjusted between 6.8 and 7.5 with 5% w/v NaOH throughout the biotreatment by a peristaltic pump. Then the effluent was pumped to the IBR, entering through a T-joint at the bottom, and water was sprayed up through the packed rings. The recirculation flow rate between the conditioner tank and the IBR was set at $1.2 \text{ m}^3 \text{ h}^{-1}$ and the neutralised pre-treated effluent was continuously pumped from the neutralisation tank to the conditioner tank by a centrifugal pump ($0.6\text{-}2 \text{ m}^3 \text{ day}^{-1}$). Once stationary state was reached between the conditioner tank and the IBR, the completely treated effluent (DOC between $40\text{-}60 \text{ mg L}^{-1}$, characteristic biological system end values for such industrial wastewater) was continuously discharged from the IBR.

During continuous biological operation, in which dissolved oxygen was kept between $4\text{-}6 \text{ mg L}^{-1}$, it was possible to calculate the volumetric gas (air)-liquid oxygen transfer coefficient (K_{La}), a characteristic parameter commonly used in the description of aerobic biological reactors, using automatic data acquisition. During this stage, dissolved oxygen clearly showed two-step consumption-absorption cycles, which made it possible to find K_{La} from the liquid-phase oxygen mass balance (Equation (2)).

$$\left(\frac{dC_L}{dt}\right) = K_L a(C_S - C_L) - x \cdot q_{O_2} \quad (2)$$

Where dC_L/dt is the oxygen accumulated in the liquid phase, $K_L a(C_S - C_L)$ is the gas-to-liquid oxygen transfer rate, C_S is the concentration of oxygen in saturated conditions (8 mg L^{-1}), C_L is the concentration of oxygen in the liquid phase at time t , x is the biomass concentration and q_{O_2} is the specific oxygen consumption.

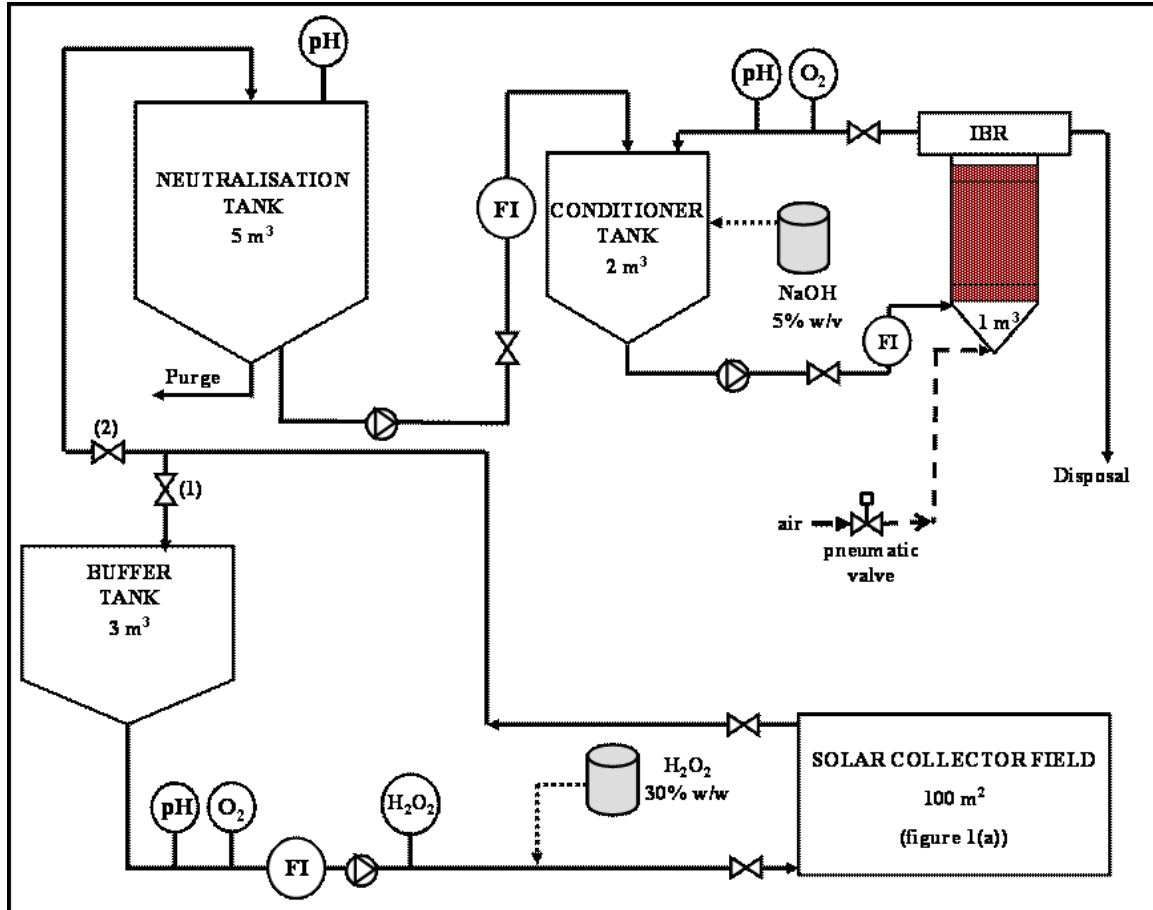


Figure 2. Simplified flow diagram of the demonstration combined photo-Fenton/aerobic biological plant.

3. RESULTS AND DISCUSSION.

3.1. Solar photo-Fenton treatment.

Prior to the combined photo-Fenton/biological treatment of MPG dissolved in an industrial wastewater, several studies had been performed to compare the pilot plant results (kinetics, hydrogen peroxide consumption, illumination time), with those from the pre-industrial-scale plant. The non-biodegradable compound²⁸, MPG, was always dissolved in wastewater received from the pharmaceutical company where the demonstration plant was erected. This company uses sea water as process water so the wastewater is highly saline (for composition see Section 2.1). It is important to note that the MPG concentration of around 600 mg L^{-1} corresponded to a DOC of 393 mg L^{-1} , but DOC for the total mixture (MPG + wastewater) was around $400\text{-}600 \text{ mg L}^{-1}$. The DOC of the industrial wastewater changed continuously depending on the ongoing factory process, but it was always approximately between 20 and 200 mg L^{-1} .

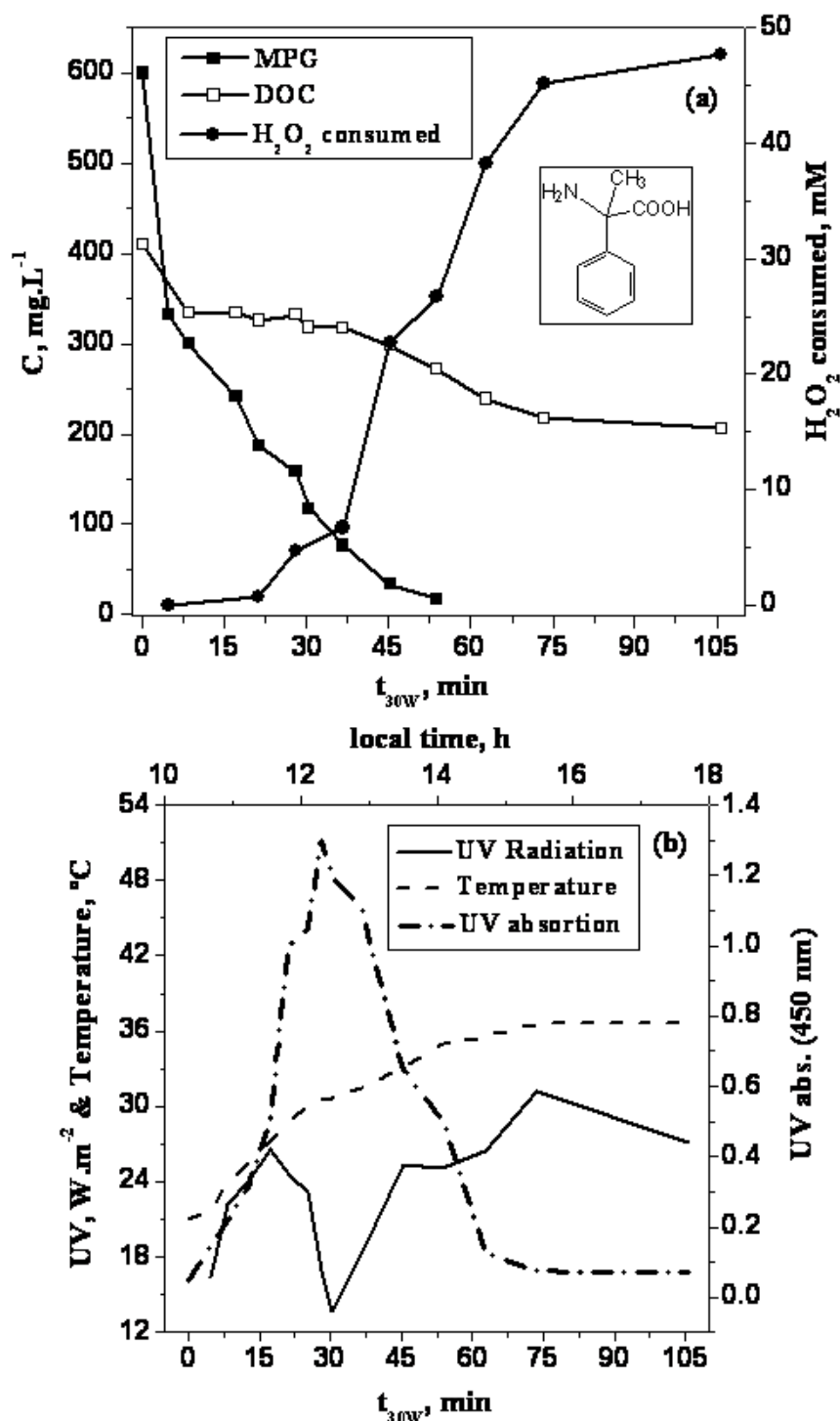


Figure 3. (a) Degradation and mineralization of MPG dissolved in saline industrial wastewater by photo-Fenton with 20 mg L⁻¹ of Fe²⁺. Hydrogen peroxide consumption is also shown. (b) Temperature and global UV radiation during the experiment.

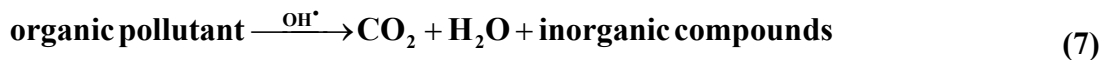
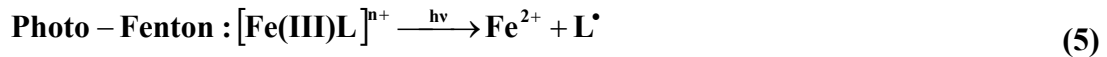
Figure 3 (a) shows the degradation and mineralization of MPG dissolved in the industrial wastewater. The complete disappearance of MPG was attained after $t_{30W} = 54$ minutes of photo-Fenton treatment ($\text{Fe}^{2+} = 20 \text{ mg}\cdot\text{L}^{-1}$) and DOC mineralization continued until $t_{30W} = 105$ min, at which moment the mixture was biodegradable, as demonstrated in previously published pilot-plant-scale studies^{26,27}. Quick decay of MPG and DOC at the beginning of the test (from $t_{30W} = 0$ to approximately $t_{30W} = 10$ minutes)

was also observed. This decay was attributed to the formation of large amounts of foam from the carbon dioxide bubbles produced by pH adjustment at the beginning of the test ($\text{pH}_0 = 2.3\text{-}2.5$). This foam retained large quantities of MPG and as foam disappeared during the photo-Fenton treatment, MPG redissolved. This strong decay may also have been caused by the Fenton reaction, as during the first minutes of the process it was governed mainly by Reaction 3, when the elimination of MPG was very fast. However, it was not possible to differentiate clearly between the disappearance of MPG retained by the foam or degraded by the Fenton reaction. In any case, it could be surmised that if 76 mg L^{-1} of DOC have been eliminated (from 410 mg L^{-1} to 334 mg L^{-1}), the corresponding MPG concentration should be 116 mg L^{-1} , but 267 mg L^{-1} of MPG actually disappeared from the water (Figure 3 (a)). It should be remarked that during the first minutes of the process, mineralization should be very slow, as at the beginning of AOPs, organics are oxidised to other degradation products, but not mineralised. Therefore, the 76 mg L^{-1} of the above-mentioned DOC eliminated corresponding to 116 mg L^{-1} of MPG must all be retained in the foam. Therefore, 464 g of MPG were retained in the foam. This means that 151 mg L^{-1} were really decomposed (but not mineralised) during the first minutes of the treatment, mainly by Reaction 4. Once the Fe^{2+} was oxidised to Fe^{3+} the process was governed mainly by the slower Reaction 5 and Fe^{3+} reduction thermal reactions (Reaction 6) (see also comments in Section 2.3.1).

The kinetics of MPG degradation has also been studied assuming that the reaction between the $\bullet\text{OH}$ radicals and the pollutant is the rate-determining step. MPG degradation may be described as a first-order reaction (Equation 3):

$$r = k_{OH} [\bullet\text{OH}]C = k_{ap}C \quad (3)$$

Where C is the MPG concentration, k_{OH} is the reaction rate constant, k_{ap} is a pseudo first-order constant, and $[\bullet\text{OH}]$ is considered constant. This was confirmed by the linear behaviour of $\ln(C_0/C)$ as a function of t_{30w} . The kinetic parameters found for MPG degradation are $k_{ap} = 0.07 \text{ min}^{-1}$ and the initial reaction rate is $r_0 = 44.4 \text{ mg L}^{-1} \text{ min}^{-1}$ ($R^2 = 0.98$). This is much lower than in the pilot-plant tests with MPG dissolved in pure sea water ($k_{ap} = 0.16 \text{ min}^{-1}$ and $r_0 = 84.0 \text{ mg L}^{-1} \text{ min}^{-1}$)²⁶. This is because, on one hand, the MPG was dissolved in an industrial wastewater containing other unknown organics ($20\text{-}200 \text{ mg DOC L}^{-1}$) which were rivals of MPG for $\bullet\text{OH}$ radicals and therefore, degradation of MPG was slower than when dissolved in pure sea water. On the other hand, the formation of large amounts of foam caused the same effect of retarding pollutant elimination by retaining MPG, which then leached out slowly (as explained above). Therefore, in industrial wastewater, the formation of foam could be highly detrimental to any AOP and should always be taken into account.



In all the pre-industrial-scale experiments performed, the required amount of hydrogen peroxide was added at the beginning of the process, as it has been demonstrated in pilot-plant tests to be the technically simplest dosing option for this industrial wastewater. Three different ways of dosing H₂O₂ for the treatment of wastewater containing MPG had been studied at pilot-plant scale²⁶: (i) the whole amount added at the beginning of the experiment, (ii) maintaining the H₂O₂ concentration at 50 mg L⁻¹ and, (iii) at 400 mg L⁻¹. An automatic PI feedback-control H₂O₂ dosing system was used to keep the H₂O₂ at a predefined concentration. The results showed a similar reaction rate with all three options. This was probably due to the fact, that in this particular case, the intermediate degradation products were strongly coloured (see Figure 1 (left)), which provoked some inner filter effect towards the dissolved iron, that is, because of the absorption of the wastewater, the photochemical reactions involving dissolved iron were inhibited. Hence, the photochemical reduction of Fe³⁺ to Fe²⁺ was hindered in the catalytic iron cycle (Reaction 5) and parallel thermal reduction reactions of Fe³⁺ gained in importance (formation of [Fe(III)(HO₂)]ⁿ⁺ complex). These thermal reactions became the main reaction pathway for the rate-limiting reduction of Fe³⁺, so a low hydrogen peroxide concentration negatively affected the overall degradation rate. When wastewater lost colour, the photo-reduction of Fe³⁺ complexes again became the rate-limiting step, as clearly seen in Figure 3 (b).

Based on the results explained above, the technically simplest solution was used for all the demonstration plant experiments. Otherwise, the concentration of H₂O₂ was always measured at the end of each photo-Fenton test in order to ensure its complete consumption during the process. The consumption of hydrogen peroxide during photo-oxidation is also shown in Figure 3 (a). The mass balance of the MPG degradation reaction is based on Reactions 7-9, where the combination of the mineralisation reaction (Reaction 7) and the decomposition of hydrogen peroxide (Reaction 8) are shown. According to Reaction 9, 72 mM of hydrogen peroxide should be consumed to mineralise 600 mg L⁻¹ of MPG, while 27 mM of hydrogen peroxide must be consumed for complete disappearance of the parent compound (Figure 3 (a)). When MPG was decomposed, a large amount of the organic content of MPG still remained in the water in the form of more oxidised organic compounds. It is worth mentioning that the demonstration-scale H₂O₂ consumption (27 mM) necessary for complete MPG degradation was similar to pilot-plant scale²⁶ (30-35 mM, 520 mg L⁻¹ of MPG), although the ratio of g H₂O₂ consumed to g MPG degraded is one and a half times lower in the demonstration plant (1.5 g H₂O₂ g MPG⁻¹) than in the pilot plant experiments (2.5 g H₂O₂ g MPG⁻¹). From Reaction 8 it may be demonstrated that the nitrogen present in the MPG molecule was released mainly as ammonium (approximately 4 mM), which increased the solution pH from 2.3-2.5 at the beginning to 2.9 at the end of the treatment. The initial pH was therefore lower (2.3-2.5) than optimal for Photo-Fenton tests (2.8-2.9), avoiding Fe³⁺ precipitation at pH higher than 3.

Temperature in the demonstration plant rises from dawn to become almost constant around afternoon, and decreases again during the evening ($t_{30W} = 0$ was around 10:30 and $t_{30W} = 105$ min was around 17:00). In Figure 3 (b), it may be observed how water temperature varied from 21 to 37°C, at the same time global UV irradiation increased from 16 W m⁻² to 30 W m⁻² (partly cloudy from 12:00 to 13:30). Under these conditions, the photo-Fenton reaction rate varied during the treatment. Other authors have described²⁹ differences of up to five times between 20 and 40°C. In recent work

with model waste water by our group³⁰, we found a similar effect (2.5 times faster at 35°C than at 20°C). It should also be mentioned that as temperature control is not economically feasible in a large-size solar photocatalytic plant, the effect of temperature and not just variation in solar UV power on the photo-Fenton reaction rate should be taken into account. This could lead to difficulties in the design of an adequate control system (for example, in determining the treatment time necessary before discharging to the biotreatment as a function of UV power and temperature) for solar photo-Fenton photocatalytic plants.

3.2. Immobilised Activated-Sludge biotreatment.

Before beginning treatment of industrial wastewater containing MPG with the combined solar photo-Fenton / aerobic biological plant, the IBR must be equipped for biomass degradation of the photo-Fenton by-products. Optimal biological system conditions for continuous treatment of pre-oxidised effluents were implemented in batch mode. Based on previous studies^{31,32}, the IBR was inoculated with 1.5 m³ of concentrated activated sludge from the aerobic tank of the pharmaceutical company's wastewater treatment plant and suspended in wastewater with a DOC of around 160 mg L⁻¹ and an ammonia concentration of 98 mg L⁻¹. Recirculation was then maintained between the conditioner tank and the IBR for several days in order to ensure optimum fixation of the sludge on the polypropylene Pall[®] Ring supports (batch mode operation). The total suspended solids (TSS), DOC, ammonium and nitrate concentrations were measured daily. The TSS analysis assessed bacteria fixation on the supports during IBR inoculation. In approximately eight days TSS = 0, so proper bacteria fixation was assured. At that moment, the normal influent from the factory wastewater treatment plant was added to the IBR in order to nourish and increase the biomass concentration fixed on the supports, and to favour the growth of a bacteria population specific to the pharmaceutical company's wastewater treatment plant. Two 1.5 m³ doses of 130 mg DOC L⁻¹ (31 mg L⁻¹ of total nitrogen) and 260 mg DOC L⁻¹ (62 mg L⁻¹ of total nitrogen) respectively, were added. In both cases DOC was degraded down to a constant 60-65 mg L⁻¹ (in approximately two days), which is typical of background noise from physiological bacteria activity in industrial wastewater biological treatment. Furthermore, the nitrification process was working properly as practically no ammonium was detected (0.3 mg L⁻¹) at constant low DOC. Therefore, correct bacteria fixation and biomass activity were proven.

Before starting continuous mode operation in the biological reactor, 0.5 m³ of the system volume was replaced by the photo-Fenton pre-treated effluent twice (DOC = 210 mg L⁻¹) in order to accustom bacteria to it, and avoid shock reducing future biomass activity. According to previous lab and pilot-plant-scale biological tests performed^{26,27}, biodegradability enhancement of industrial wastewater containing MPG by photo-Fenton (Fe²⁺ = 20 mgL⁻¹) was accomplished when MPG was completely eliminated and DOC was reduced to approximately 50% of the initial value (see Figure 3 (a)). Therefore, the photo-Fenton treatment was continued in the demonstration plant to the same level (i.e., MPG completely degraded, 50% of initial DOC, t_{30W} = 105 min), at which point, the pre-oxidised effluent was transferred to the neutralisation tank (see Figure 2) where the pH was manually adjusted to 7. Then, the biological system was drained and refilled twice with the effluent, where the DOC fell to the desired value (around 60 mg L⁻¹, and TSS = 0) after around 4 or 5 days of biotreatment in batch mode. No mineral medium was added to the photo-Fenton pre-treated effluent as the sea water matrix and the amount of ammonium generated from the degradation of MPG

(approximately 4 mM), fulfilled the required C and N, P (8-10 mg/L depending on wastewater composition), Fe (from photo-Fenton) and Ca ratios for conventional biological systems as published elsewhere³³: C:N:P of 100:20:5 and C:Fe:Ca of 100:2:2. Moreover, the demonstration biological plant was intended to simulate a real wastewater treatment plant based on supported biomass, so therefore, no additional mineral solution was used so conditions would be as realistic as possible. That is also the reason why inoculation and maintenance of activated sludge in the IBR was carried out under the same conditions as in the pharmaceutical company's wastewater treatment plant.

3.3. Combined solar photo-Fenton-aerobic biological system.

Once demonstrated that the Immobilised Activated Sludge was able to eliminate the remaining DOC from the photo-Fenton pre-treated wastewater containing MPG, semi-continuous operation of the combined system began. Solar photo-Fenton treatment was always performed in batch mode, while the biological reactor was operated continuously. This meant that several photo-Fenton batches were carried on under the same conditions shown in Figure 3 and fed to the neutralisation tank, from which the effluent was continuously pumped to the conditioner tank and through the IBR. As explained in Section 2.3.2., in stationary-state conditions, the completely treated effluent (at DOC around 60 mg L⁻¹, TSS = 0) was continuously discharged from the IBR at the same flow rate as the inlet from the neutralisation tank.

Figure 4 shows the specific volumetric organic load to the IBR, the DOC removed in the biological treatment and the variations in continuous flow (from 0.6 to 2 m³ day⁻¹). The DOC load and the DOC removed are calculated taking into account the continuous inlet flow (L day⁻¹), inlet DOC (g m⁻³), outlet DOC (g m⁻³) and the volume occupied by Pall ring® supports in the IBR (0.7 m³), which is a volume representative of the amount of active biomass in the reactor.

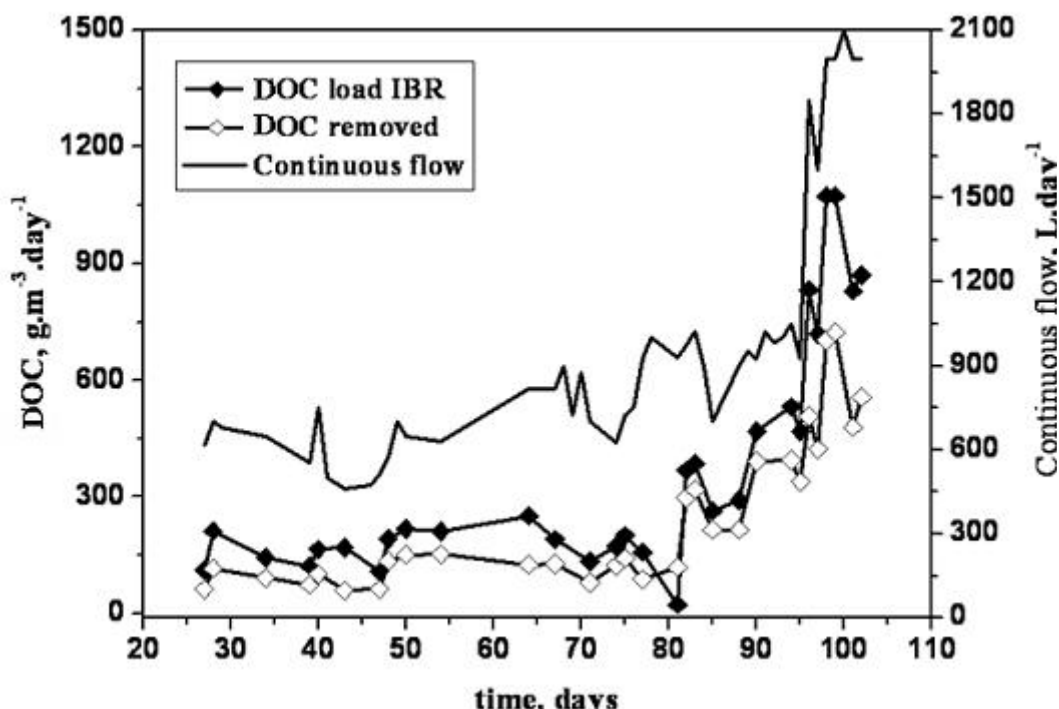


Figure 4. Specific volumetric organic load of IBR, continuous flow from the neutralisation tank to the conditioner tank and DOC removed per m³ occupied by polypropylene supports in the IBR.

The biological system started to operate in continuous mode on Day 21, and until Day 81 (600-800 L day⁻¹ from Day 21 to 64), the specific volumetric organic load of the IBR always remained around 200 g m⁻³ day⁻¹. From Day 64 to 95, it was attempted to keep the continuous flow from the neutralisation tank to the conditioner tank between 800 and 1000 L day⁻¹. After Day 81 the initial MPG concentration dissolved in the industrial wastewater was raised to 1 g L⁻¹ previous to the photo-oxidation step to achieve significantly higher organic loads in the IBR (from 360 to approximately 1000 g m⁻³ day⁻¹) without having to increase the number of batch treatments in the solar photo-Fenton stage proportionally. These photo-Fenton batches required more hydrogen peroxide (35 L, corresponding to a 77 mM concentration) at the beginning of the process and a longer illumination time ($t_{30w} = 180$ min), to enhance the biodegradability of the pre-treated effluent (removal of 50% of initial DOC). Finally, from day 95 to 100, the continuous flow was doubled to 2000 L day⁻¹ in only five days. This last 20-day stage from Day 80 to 100 made it possible to determine the biological system's maximum treatment capacity. As observed from Figure 4, the amount of DOC removed in the biological system could generally said to be around 2/3 of the incoming DOC.

Figure 5 shows DOC and nitrogen concentrations (from NH₄⁺) in the IBR outlet during continuous operation of the biological system. It is important to observe how outlet DOC remained between 55 and 70 mg L⁻¹ until day 90 (within the limits for background noise from industrial wastewater bacteria activity), but from this point to the end, DOC in the outlet increased to 110-120 mg L⁻¹. At that moment, the specific volumetric organic load was more than doubled (470 g m⁻³ day⁻¹). There are two possible reasons for this increase in DOC, either the heterotrophic bacteria had reached the limit of their capacity and therefore, outlet DOC rose, or the more concentrated inlet contained more non-biodegradable substances. In order to find out which of these two assumptions was true, after Day 102 a batch was run with no further additions. During approximately 12 days of batch recirculation between the conditioner tank and the IBR, the DOC in the system gradually fell to around 84 mg L⁻¹. This indicates that less degradation by the photo-Fenton treatment to increase the organic load fed to the IBR caused more hardly biodegradable compounds to be formed. It is worth remarking that DOC outlet concentration depends not only on the biodegradability of the effluent, but also on the dimensioning of the biological plant and the mean residence time inside the biological reactor. The mean residence time in the immobilised activated sludge bio-reactor studied in this work was approximately 17 hours when operating at 1 m³ day⁻¹ (day 27 – 95) and 8 hours at 2 m³ day⁻¹ (day 95 – 102). In this sense, the increase in the DOC outlet demonstrated the need to scale up slightly the bio-treatment to make the residence time in the biological reactor longer and allow fixed biomass to also degrade hardly biodegradable by-products from photo-Fenton treatment. It is therefore indispensable to thoroughly optimise these points for each real-size plant design based on the specific wastewater to be treated. In the particular case of the demonstration plant and the real wastewater specifically tested in this work, maximum specific volumetric DOC degradation was found to be approximately 500 g m⁻³·day⁻¹ (Figure 4), which was more than three times higher than at pilot plant scale, mainly due to the strong increase in the amount of active biomass in the demonstration plant.

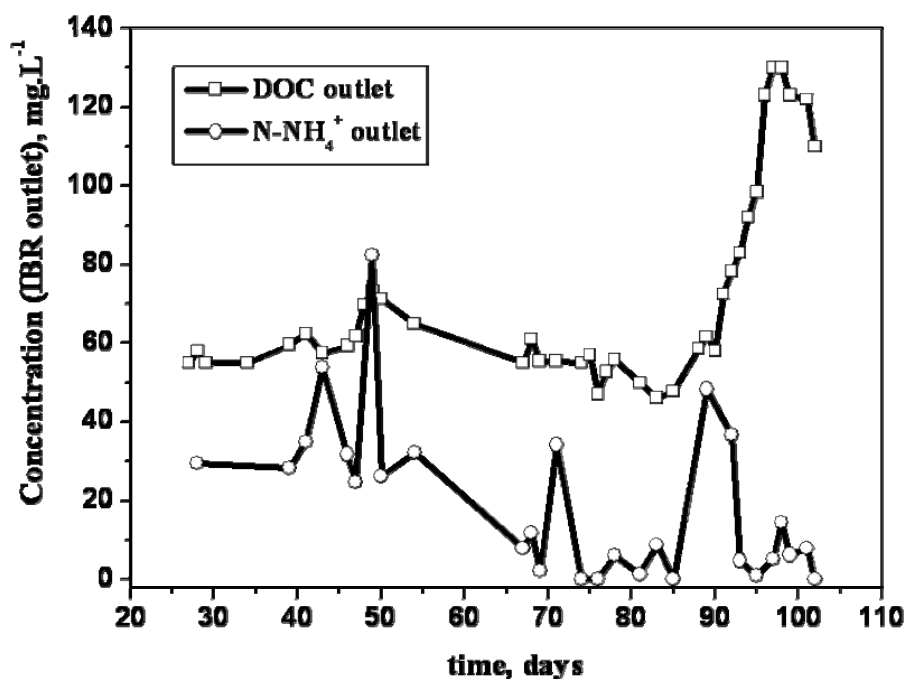


Figure 5. DOC and nitrogen from NH_4^+ in the IBR outlet during continuous operation.

Another important point in the aerobic biological treatment is that ammonia concentration in the effluent dropped, especially when the wastewater contained large amounts of NH_4^+ . MPG contains 8.5% nitrogen and its degradation intermediates in pre-treated water would contain part of it. As mentioned in Section 3.1, nitrogen from the MPG molecule was released mainly as NH_4^+ , and the wastewater in which MPG was dissolved also contained NH_4^+ . The nitrogen from ammonium in the IBR outlet is also plotted in Figure 5 where it can be observed that, from the first day to Day 71, the nitrogen concentration was between 30-40 mg L^{-1} occasionally rising to 70 mg L^{-1} . During this phase of continuous operation, automatically controlled dissolved oxygen in the IBR was kept between 4-6 mg L^{-1} (see control description in Section 2.3.2), according to the pilot-plant experiments²⁶. However, contrary to the pilot-plant results, in the demonstration plant, dissolved oxygen control was problematic, mainly because the air diffusers (at the bottom of the IBR) occasionally got plugged up when aeration stopped because the upper limit of oxygen concentration was reached. Consequently, air pressure had to be raised to unplug the air diffusers, causing violent bubbling through the immobilised biomass zone, and fixed biomass came unattached. Furthermore, the most common reasons for the increase in residual NH_4^+ concentration are inhibiting substances, insufficient aeration and temperature too high. Temperatures in the IBR were never above 29°C, so it was not this parameter that was causing the problem. Therefore, automatic control of the dissolved oxygen was discontinued and was kept saturated (8 mg L^{-1}) in the IBR from Day 71 to the end of continuous operation. This situation was not economically optimised. Only when the specific volumetric organic load increased did the concentration of nitrogen rise, but after four days of biomass adaptation, ammonia concentration fell again.

As mentioned at the end of Section 2.3.2., during continuous biological operation it was possible to calculate the volumetric oxygen transfer coefficient (K_{La}), because to the automatic control of dissolved oxygen kept it at 4-6 mg L^{-1} . Since aeration is stopped in the consumption phase and the oxygen transfer rate becomes null ($K_{La}(C_s - C_L) = 0$), solution of Equation 8 using the least squared error to fit the data gave a K_{La} of

20±5 h⁻¹. This result is similar to those found for fluidized bed bioreactors with 1 vvm (volume per minute) and in stirred tank bioreactors at 400 rpm³⁴. Such bioreactors are widely employed in biological systems for different purposes. Furthermore, continuous dissolved oxygen measurements showed that it always remained between 2 and 8 mg L⁻¹ when the automatic control was switched to continuous air supply. In fact, when the organic load was increased, the concentration of dissolved oxygen was always in that range. Otherwise, due to the polypropylene support packing inside the IBR, dissolved oxygen transfer in the column was not homogenous, and air bubbles would have to have preferred ways.

Finally, when the continuous flow was increased to 2 m³ day⁻¹, around 40 mg L⁻¹ of NO₂⁻ was detected, showing that the system was not working properly. Considering that not only must DOC be degraded by the bio-treatment, but ammonia concentration must also be decreased, the final specific volumetric DOC degradation in the IBR (500 g m⁻³ day⁻¹) is the maximum treatment capacity for this demonstration plant under specific pre-treatment effluent conditions. Figure 6 shows the percentage of overall DOC removed by each step of the combined solar photo-Fenton / aerobic biological process, equivalent to the percentage of the initial DOC (100%) degraded in each step. Overall efficiency was in the range of 85-95% elimination of initial DOC, of which 50-65% was removed in the solar photo-Fenton treatment and 20-45% in the immobilised activated-sludge bio-treatment. It should also be mentioned that overall degradation efficiency depends not only on oxidation degree but also on the DOC inlet concentration.

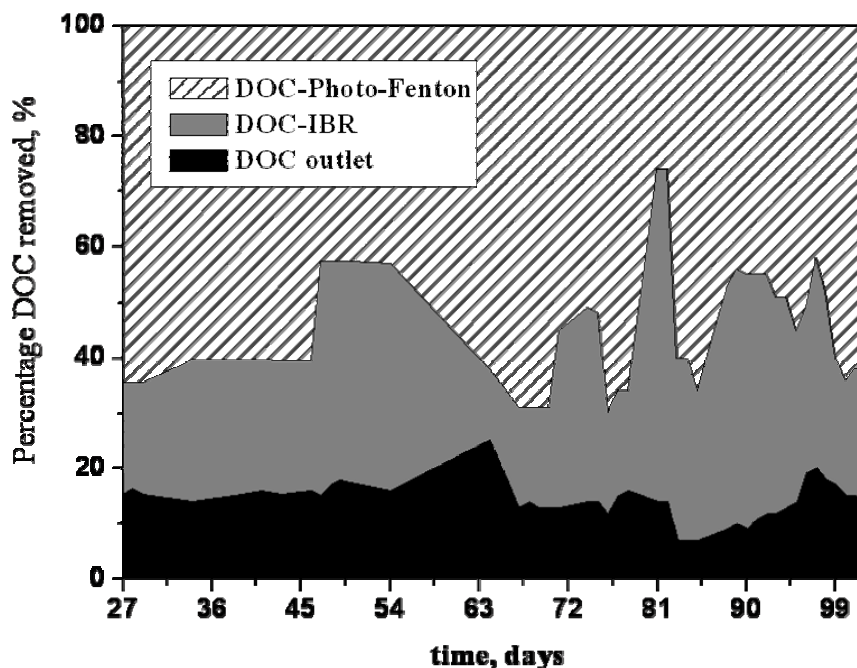


Figure 6. Percentage of DOC removed by photo-Fenton and by biological treatment (IBR). The percentage of DOC remaining in the IBR outlet is also shown.

4. CONCLUSIONS.

Compared to previously published pilot-plant-scale results for treatment of this saline industrial wastewater^{26,27}, demonstration solar photo-Fenton pre-treatment successfully enhanced the biodegradability of the effluent in a reasonable length of time ($t_{30w} = 105$ min). In view of the difficulties for very precise demonstration-plant scale testing, it should be mentioned that pilot plant tests are indispensable for accurate large-scale

design parameters and operating procedures. It is also important for the demonstration plant to be constructed using a photoreactor design as similar as possible to the pilot plant so that results can be extrapolated. This is even more important with solar irradiation, as the source of energy is not constant.

The aerobic biological treatment was then able to reduce the DOC from the pre-oxidised effluent to specific bacteria activity ($60\text{--}65\text{ mg L}^{-1}$) by means of saline activated sludge fixed on propylene Pall ring® supports. The maximum specific volumetric DOC degradation in the biological treatment of the wastewater studied in this work was found to be $500\text{ g m}^{-3}\text{ day}^{-1}$ when a continuous flow rate of $2\text{ m}^3\text{ day}^{-1}$ was maintained.

This two-step field treatment was operated in semi-continuous mode (solar photo-Fenton treatment in batch mode and the biological process in continuous mode), and overall efficiency was in the range of 85-95%, of which 50-65% was removed in the solar photo-Fenton treatment and 20-45% in the immobilised activated-sludge bio-treatment. It may therefore be concluded that the following points must be taken into account in future actual-size plants optimized for a specific industrial wastewater:

- a. Foam formation must be considered highly detrimental to apply photo-Fenton process.
- b. Apart from variation in solar UV power, temperature also affects the photo-Fenton reaction rate and should be taken into account in designing solar photocatalytic plant control systems.
- c. In the biological treatment, increased outlet organic content demonstrates the need of scaling up the bio-treatment by lengthening the residence time in the biological reactor to allow the fixed biomass to degrade part of the recalcitrant biodegradable photo-Fenton by-products.

5. REFERENCES.

- [1] Gogate, P.R., Pandit, A.B. A review of comparative technologies for wastewater treatment I: oxidation technologies at ambient conditions. *Adv. Environ. Res.* **2004**, 8, 501.
- [2] Gogate, P.R.; Pandit, A.B. A review of comparative technologies for wastewater treatment II: Hybrid methods. *Adv. Environ. Res.* **2004**, 8, 553.
- [3] Devipriyas, S.; Yesodharan, S. Photocatalytic degradation of pesticide contaminants in water. *Sol. Energy Mater. Sol. Cells.* **2005**, 86, 309.
- [4] Herrmann, J.M. Heterogeneous photocatalysis: state of the art and present applications. *Top. Catal.* **2005**, 14(1-4), 48.
- [5] Pera-Titus, M.; García-Molina, V.; Baños, M.A.; Giménez, J.; Esplugas, S. Degradation of chlorophenols by means of advanced oxidation processes: a general review. *Appl. Catal. B: Environ.* **2004**, 47, 219.
- [6] Andreozzi, R.; Caprio, V.; Insola, A.; Marotta, R. Advanced oxidation processes (AOP) for water purification and recovery. *Catal. Today.* **1999**, 53, 131.
- [7] Malato, S.; Blanco, J.; Vidal, A.; Richter, C. Photocatalysis with solar energy at a pilot-plant scale: an overview. *Appl. Catal. B: Environ.* **2002**, 37, 1.
- [8] Bahnemann, D. Photocatalytic Water Treatment: Solar Energy Applications. *Sol. Energy.* **2004**, 77, 445.
- [9] Goswami, D.Y.; Vijayaraghavan, S.; Lu, S.; Tamm, G. New and emerging developments in solar energy. *Sol. Energy.* **2003**, 76, 33.
- [10] Blanco, J.; Fernández, P.; Malato, S. Solar Photocatalytic Detoxification and Disinfection of Water: Recent overview. *J. Sol. Energy Eng.* **2007**, 129, 4.

- [11] Pignatello, J.J.; Oliveros, E.; MacKay, A. Advanced oxidation processes for organic contaminant destruction based on the Fenton reaction and related chemistry. *Crit. Rev. Env. Sci. Technol.* **2006**, 36, 1.
- [12] Pulgarín, C.; Invernizzi, M.; Parra, S.; Sarria, V.; Polania, R.; Péringer, P. Strategy for the coupling of photochemical and biological flow reactors useful in mineralization of biorecalcitrant industrial pollutants. *Catal. Today.* **1999**, 54, 341.
- [13] Kositzi, M.; Poulios, I.; Malato, S.; Cáceres, J.; Campos, A. Solar photocatalytic treatment of synthetic municipal wastewater. *Water Res.* **2004**, 38, 1147.
- [14] Machado, A. E. H.; Xavier, T. P.; Rodrigues de Souza, D.; de Miranda, J. A.; Mendonça Duarte, E. T. F.; Ruggiero, R.; de Oliveira, L.; Sattler, C. Solar photo-Fenton treatment of chip board production waste water. *Sol. Energy.* **2004**, 77, 583.
- [15] Sattler, C.; Funken, K.-H.; de Oliveira, L.; Tzschirner, M.; Machado, A.E.H. Paper Mill Wastewater Detoxification by Solar Photocatalysis. *Wat. Sci. Technol.* **2004**, 49 (4), 189.
- [16] Farré, M. J.; Franch, M. I.; Malato, S.; Ayllón, J. A.; Peral, J.; Doménech, X. Degradation of some biorecalcitrant pesticides by Homogeneous and Heterogeneous Photocatalytic Ozonation. *Chemosphere.* **2005**, 58, 1127.
- [17] Oller, I.; Fernández-Ibáñez, P.; Maldonado, M.I.; Pérez-Estrada, L.; Gernjak, W.; Pulgarín, C.; Passarinho, P.C.; Malato, S. Solar heterogeneous and homogeneous photocatalysis as a pre-treatment option for biotreatment. *Res. Chem. Interm.* **2007**, 33(3-5), 407.
- [18] Esplugas, S.; Ollis, D.F. Economic Aspects of Integrated (Chemical + Biological) Processes for Water Treatment. *J. Adv. Oxid. Technol.* **1997**, 2 (1), 197.
- [19] Marco, A.; Esplugas, S.; Saum, G. How and why combine chemical and biological processes for wastewater treatment. *Wat. Sci. Technol.* **1997**, 35, 321.
- [20] Mantzavinos, D.; Psillakis, E. Enhancement of biodegradability of industrial wastewaters by chemical oxidation pre-treatment. *J. Chem. Technol. Biotechnol.* **2004**, 79, 431.
- [21] Bressan, M.; Liberatorre, L.; D'Alessandro, L.; Tonucci, L.; Belli, C.; Ranalli, G. Improved combined chemical and biological treatments of olive oil mill wastewaters. *J. Agric. Food Chem.* **2004**, 52, 1228.
- [22] Mantzavinos, D.; Kalogerakis, N. Treatment of olive mill effluents Part I. Organic matter degradation by chemical and biological processes-an overview. *Environ. Technol.* **2005**, 31, 289.
- [23] Heinzle, E.; Geiger, F.; Fahmy, M.; Kut, O.M. Integrated Ozonation-Biotreatment of Pulp Bleaching Effluents Containing Chlorinated Phenolic Compounds. *Biotechnol. Prog.* **1992**, 8, 67.
- [24] Sarria, V.; Deront, M.; Péringer, P.; Pulgarín, C. Degradation of a biorecalcitrant dye precursor present in industrial wastewaters by a new integrated iron (III) photoassisted-biological treatment. *Appl. Catal. B: Environ.* **2003**, 40 (3), 231.
- [25] Contreras, S.; Rodríguez, M.; AlMamani, F.; Sans, C.; Esplugas, S. Contribution of the ozonation pre-treatment to the biodegradation of aqueous solutions of 2,4-dichlorohydroquinone. *Wat. Res.* **2003**, 37, 3164.
- [26] Oller, I.; Malato, S.; Sánchez-Pérez, J.A.; Gernjak, W.; Maldonado, M.I.; Pérez-Estrada, L.A.; Pulgarín, C. A Combined solar photocatalytic-biological field system for the mineralization of an industrial pollutant at pilot scale. *Catal. Today.* **2007**, 122, 150.

- [27] Malato, S.; Blanco, J.; Maldonado, M.I.; Oller, I.; Gernjak, W.; Pérez-Estrada, L. Coupling solar photo-Fenton and biotreatment at industrial scale: Main results of a demonstration plant. *J. Haz. Mat.* **2007**, in press.
- [28] M. Lapertot, C. Pulgarín. Biodegradability assessment of several priority hazardous substances: Choice, application and relevance regarding toxicity and bacterial activity. *Chemosphere* 65 (2006) 682-690
- [29] Sagawe, G.; Lehnard, A.; Lüber, M.; Bahnemann D. The insulated solar Fenton hybrid process: Fundamental investigations. *Helv. Chem. Acta.* **2001**, 84, 3742.
- [30] Gernjak, W.; Fuerhacker, M.; Fernández-Ibañez, P; Blanco, J.; Malato, S. Solar photo-Fenton treatment Process parameters and process control. *Appl. Catal. B: Environ.* **2006**, 64, 121.
- [31] Sarria, V.; Denfack, S.; Guillod, O.; Pulgarín, C. An innovative coupled solar-biological system at field pilot scale for the treatment of biorecalcitrant pollutants. *J. Photochem. Photobiol., A: Chemistry.* **2003**, 159, 89.
- [32] Farré, M.J.; Doménech, X.; Peral, J. Assessment of photo-Fenton and biological treatment coupling for Diuron and Linuron removal from water. *Water Res.* **2006**, 40, 2533.
- [33] Henze, Harremoës. Wastewater treatment. Biological and Chemical Processes. *La Cour Jansen and Arvin, 3rd Ed., Springer.* **2002**.
- [34] Casas López, J.L.; Rodríguez Porcel, E.M.; Oller Alberola, I.; Ballesteros Martín, MM.; Sánchez Pérez, J.A.; Fernández Sevilla, J.M.; Chisti, Y. Simultaneous Determination of Oxygen Consumption Rate and Volumetric Oxygen Transfer Coefficient in Pneumatically Agitated Bioreactors. *Ind. Eng. Chem. Res.* **2006**, 45, 1167.